NASA TECHNICAL MEMORANDUM

NASA TM X- 71441

NASA TM X- 71441

ROLLING-ELEMENT BEARINGS - A REVIEW OF THE STATE OF THE ART

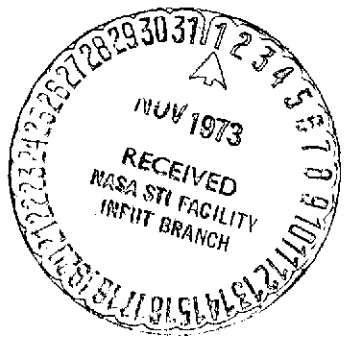

by William J. Anderson and Erwin V. Zaretsky
Lewis Research Center
Cleveland, Ohio 44135

TECHNICAL PAPER proposed for presentation at
Tribology Workshop sponsored by the National
Science Foundation
Atlanta, Georgia, October 19 - 20, 1973

ROLLING-ELEMENT BEARINGS - A REVIEW OF THE STATE OF THE ART

by William J. Anderson and Erwin V. Zaretsky

Lewis Research Center
National Aeronautics and Space Administration
Cleveland, Ohio

ABSTRACT

Some of the research conducted which has brought rolling-element technology to its present state is discussed. Areas touched upon are material effects, processing variables, operating variables, design optimization, lubricant effects and lubrication methods. Finally, problem areas are discussed in relation to the present state-of-the-art and anticipated requirements.

E-7697

INTRODUCTION

The last three decades have seen a significant increase in the severity of applications in which rolling-element bearings are expected to function reliably and with long life. Rolling-element bearings are now required to operate at much higher speeds and, to a lesser extent, higher temperatures than in the early 1940's. The increased speed and temperature requirements originated principally with the advent of the aircraft gas turbine engine. Its development, coupled with the appearance of a variety of high speed turbine driven machines, has resulted in a wide gamut of bearing requirements for mainshaft, accessory and transmission applications.

The most recent trends in gas turbine design and development have been toward engines with even higher thrust-to-weight ratios and increased power output, which result in a requirement for higher shaft speeds and

larger shaft diameters.[1][1] Bearings in current production aircraft turbine engines operate in the range from 1.5 to 2 million DN (bearing bore in millimeters times shaft speed in rpm). Engine designers anticipate that turbine bearing DN values will have to increase to 2.5 to 3 million by 1980. The effects of these design trends on rolling-element bearings will be discussed.

In support of these engines, as well as for similar high performance oriented bearing applications, a reliable bearing-lubricant system is required. Such a system requires essentially three key items. These are, a suitable lubricant, a reliable bearing structural material, and an optimized bearing design coupled with the proper operational parameters needed to sustain ultrahigh speeds. The higher temperature requirements have necessitated the development of new lubricants with better oxidative and thermal stability. The effects of these lubricants on bearing life have had to be investigated experimentally. The use of new lubricant formulations has been responsible, in part, for research on elastohydrodynamics. This has led to a better understanding of the physical phenomena that occur in Hertzian contacts. Although a complete discussion of elastohydrodynamics is beyond the scope of this paper, its immediate implications regarding bearing design will be discussed.

Classical rolling-element fatigue has always been considered the prime life limiting factor for rolling-element bearings although in actuality less than 10 percent of them fail by fatigue. With proper handling, installation lubrication and maintenance of lubrication

[1]Numbers in brackets designate References at end of paper.

system cleanliness, a rolling-element bearing will fail by fatigue. Because fatigue results from material weaknesses, research to improve material quality has been a continuing activity. The results of this research will be discussed.

Based upon the problems and criteria set forth herein above, it is the objective of this paper to review the state-of-the-art advancements in the field of rolling-element technology. Because of the extensive amount of work which has been performed over the past decade it is difficult to incorporate the entire spectrum of research performed. However, the authors will attempt to refer the reader to those pertinent references which will provide an in-depth study into particular aspects of rolling-element bearing technology. With proper definition of the technology and problems related thereto, the reader can define pertinent research which should be performed.

MATERIAL EFFECTS

Fatigue Life of Steels

There has been a considerable number of studies performed to determine the rolling-element fatigue lives of various bearing materials [2-12]. However, none of these studies maintained the required close control of operating and processing variables such as material hardness, melting technique, and lubricant type and batch for a completely unbiased material comparison. The more standard mechanical tests such as tension and compression tests or rotating beam tests are not correlatable with rolling-element fatigue results [7].

Rolling-element fatigue tests were run with eight through-hardened bearing materials at 150° F [13-15]. These materials were AISI 52100, M-1, M-2, M-10, M-42 (similar to WB-49), M-50, T-1 and Halmo. One-half inch diameter balls of each material were run in five-ball fatigue testers. Care was taken to maintain constant all variables known to affect rolling-element fatigue life. The longest lives at 150° F were obtained with AISI 52100. Ten-percent lives of the other materials ranged from 7 to 78 percent of that obtained with 52100. A trend is indicated toward decreased rolling-element fatigue life with increased total weight percent of alloying elements (Fig. 1). Three groups of 120-mm bore ball bearings made from AISI M-1, AISI M-50, and WB-49 were fatigue tested at an outer-race temperature of 600° F [15, 16]. The 10-percent lives of the M-50 and M-1 bearings exceeded the calculated AFBMA life by factors of 13 and 6, respectively. The bearings with WB-49 races showed lives less than AFBMA life. The results of the bearing tests (Fig. 2) at 600° F correlated well with the results of the five-ball fatigue data at 150° F [15].

Melting Techniques

One cause of rolling-element fatigue is nonmetallic inclusions [14, 17-19]. Basic inclusion types include sulfides, aluminates, silicates and globular oxides. These inclusions may act as stress raisers similar to notches in tension and compression specimens or in rotating beam specimens. Incipient cracks emanate from these inclusions (Fig. 3), enlarge and propagate under repeated stresses forming a network of cracks which form into a fatigue spall or pit (Fig. 4). In general the cracks

propagate below the rolling-element surface approximately 45° to the normal; that is, they appear to be in the plane of maximum shearing stress. Carter [4, 18] made a qualitative generalization that the location of an inclusion with respect to the maximum shearing stress is of prime importance. Based on observations of inclusions in AISI 52100 and AISI M-1 steels, it was concluded that:

1. Inclusion location is of primary importance;

2. Size and orientation are also important;

3. The oxides and larger carbides are more harmful than the softer sulfide inclusions; and

4. Inclusions, carbides and irregular matrix conditions appear slightly less harmful to fatigue life in SAE 52100 than in AISI M-1.

The conclusions of [4, 18] were substantiated by research reported in [20]. These results which are summarized in Fig. 5 show that as the total number of alumina and silicates increase, fatigue life decreases. However, an increase in sulfides may have a positive effect upon fatigue life. (Unpublished work which attempted to induce sulfides into bearing steels used for ball lubrication resulted in cracked ball blanks. As a result, this work was abandoned.) In addition to inclusions, material defects such as microcracks, trace elements or unusual carbide formations present in the material can contribute to failure.

One method for increasing rolling-element reliability and load capacity is to eliminate or reduce nonmetallic inclusions, entrapped gases, and trace elements. Improvements in steel-making processing, namely melting in a vacuum, can achieve this.

Induction vacuum melting (IVM) is the term applied to a process in which a cold charge is melted in an induction furnace and subsequently poured into ingots, the whole operation being performed while the melt is exposed to vacuum. This process is illustrated in Fig. 6. The drawbacks of this process are a wide variation in quality and a substantial price premium. Refractory problems cause the quality variations, and the premium price is due to the fact that the equipment is necessarily small, and production is in small tonnages [21, 22].

A more improved method of making bearing steel is consumable-electrode vacuum melting. This process, normally referred to as CVM, is a technique wherein electrodes made from a primary air-melted heat are remelted by an electric arc process. The product thus remelted solidifies in a water-cooled copper mold under vacuum as shown in Fig. 7. This gives completely different solidification conditions from the induction vacuum melt technique. This process produces a much more consistent high-quality steel [22].

It is possible with any of these melt techniques to produce material with a lower inclusion content than air-melted material, particularly those inclusions which are generally considered to be more injurious, such as oxides, silicates, and aluminates. These inclusions are, in part, the result of standard air melt deoxidation practice which involves the use of silicon and aluminum. Exposing the melt to a vacuum permits deoxidation to be performed effectively by the carbon. The products formed when using carbon as a deoxidizer are gaseous, and thus are drawn off in the vacuum. Further, these techniques permit extremely close control of chemistry and also permit production of variations in chemical analysis which was at one time impractical.

Fatigue tests of 6309-size deep-groove ball bearings made from two heats of AISI M-50 material produced by consumable vacuum-melting processes resulted in an average 10-percent life of 4.2 times the catalog life of 10 million revolutions. Additional fatigue tests of the same type of bearings made from a single heat of air melted M-50 material resulted in a life of only 0.4 times the catalog rating [23].

The improvement in life of bearings made of vacuum-melted steels does not appear to be commensurate with the improvement in cleanliness. This, of course, upholds the long-held theory that cleanliness is not the only factor involved in bearing fatigue. Even in exceptionally clean materials, nonmetallics are present to some degree and, depending on the magnitude and location in relation to the contact stresses, can be the nucleus of fatigue cracks as previously discussed. A single heat of primary air melted AISI 52100 steel was processed through five successive consumable electrode vacuum remelting cycles. Groups of 6309-size bearing inner-races were machined from material taken from the air-melt ingot and the first, second and fifth remelt ingots for evaluation; they were then heat treated and manufactured as a single lot to avoid group variables. With each remelt, a progressive reduction of nonmetallic content occurred. Endurance results, summarized in Fig. 8, show that the 10-percent life appears to increase for successive remelting with the fifth remelt material reaching a life approximately 4 times that of the air melt group [24].

Double vacuum-melted (IVM-CVM) AISI M-50 steel is commercially availalbe. This material is processed with the first heat being induction vacuum melted. The material is subsequently consumable-electrode vacuum

melted. Tests with 120-mm bearings made from IVM-CVM AISI M-50 steel [25] indicated that this material may produce fatigue life at least five times that achieved by normally processed CVM AISI M-50 steel.

Hardness Effects

Heat treatment can significantly influence several rolling-element bearing material properties. Most bearing procurement specifications do not designate heat treatment but rather call for certain material characteristics such as grain size and hardness, which are controlled by the heat treat cycle. Hardness is the most influential heat treat induced variable in rolling-element fatigue [7, 11, 26]. A relationship has ben proposed in [27] which approximates the effect of bearing material hardness on fatigue life.

$$L_2/L_1 = e^{m(R_{c2} - R_{c1})} \tag{1}$$

where L_1 and L_2 are the bearing ten-percent life at bearing hardnesses of R_{c2} and R_{c1}, respectively, and m is a material constant. It is assumed for the purpose of this relationship which was obtained for AISI 52100 that all components in the rolling-element bearing, that is rolling elements and races, are of the same hardness. It was further assumed that this equation can be extended to high-speed tool steels.

Hot hardness measurements were made for groups of AISI 52100, Super Nitralloy, AISI M-1, AISI M-50, Halmo, WB-49, Matrix II, WD-65 and modified AISI 440-C [28-30]. The results of these hardness measurements are shown in Fig. 9. These normalized data show that regardless of the initial hardness, the hot hardness of the individual materials shows the same functional dependence. That is, the charges in hardness with increasing

temperature are all independent of initial hardness.

The data of Fig. 9 when plotted on log-log corrdinates [30] can be represented by a straight line having the form

$$(Rc)_T = (Rc)_{RT} - \alpha \Delta T^{\beta} \tag{2}$$

where

$(Rc)_T$ = Rockwell C hardness at operating temperature

$(Rc)_{RT}$ = Rockwell C hardness at room temperature

ΔT = change in temperature, $T_T - T_{RT}$

T_T = operating temperature, deg F

T_{RT} = room temperature, deg F

α = temperature proportionality factor, $(\text{deg F})^{-\beta}$

β = exponent

From equation (1), let L_1 be the bearing life calculated according to [31]. Hence

$$L_1 = \left(\frac{C}{P}\right)^n \tag{3}$$

where C is the basic load rating of the bearing and P is the equivalent load [31]. Assume, based upon experience, that the basic load rating is based upon a material hardness of Rockwell C60. As a result, equation (1) can be written

$$L_2 = e^{m[(Rc)_T - 60]} \left(\frac{C}{P}\right)^n \tag{4}$$

Combining equations (2) and (4) where $T_{RT} = 70$ deg F,

$$L_2 = e^{m\{[(Rc)_{RT} - 60] - \alpha(T_T - 70)^{\beta}\}} \left(\frac{C}{P}\right)^n \tag{5}$$

From the above equation, the life of a rolling-element system can be determined as a function of room temperature hardness and operating temperature for a particular steel.

Carbide Effects

From the data of [13-15] it was speculated that an interrelation existed among median residual carbide size, number of residual carbide particles per unit area and the percent area of residual carbides and rolling-element fatigue life. Residual carbides are those carbides that do not go completely into solution during austenitizing and are a function of the alloying elements and heat treatment. This is opposed to the hardening carbide precipitates, which precipitate upon aging at the tempering temperature. The carbides referred to in the following will be the residual carbides.

If the carbides in a material are the nucleation site of an incipient fatigue failure, then the probability of survival S for a lot of specimens or a single specimen can be expressed as a function of three variables (a) percent area of carbides, a, (b) median carbide size (length), m, and (c) total number of carbides per unit area, n [30, 32]. Based upon a statistical analysis a carbide factor C' can be derived where

$$C' = \frac{L_3}{L_2} \tag{6}$$

In [13-15] AISI 52100 is the material which produced the highest life values. Therefore, the values for the carbide factor C' can be normalized with respect to the AISI 52100 material. Thus,

$$C' = \frac{1}{K_1\left(\frac{m}{0.26} + \frac{718}{n} + \frac{\alpha}{9.54} + \frac{K_4}{K_1} Co\right)} \tag{7}$$

From experimental data, K_1 and K_4 were empirically determined to be 1/3 and 4/3, respectively [30, 32].

In Fig. 10 the relative material L_{10} lives are plotted against the carbide factor C'. (The L_{10} life is that time at which there is a 90 percent probability of survival for a bearing or group of bearings.) There appears to be a reasonable correlation between the carbide factor C and relative life. For the individual groups of data and the combined groups the confidence number was found to be 0.87 and 0.83, respectively. This means that the carbide factor C can give a reasonable prediction of relative life under identical conditions of material hardness and lubrication mode. Thus, the carbide parameter seems to transcend such variables as heat treatment, chemical composition, and hardening mechanism to predict the lives of individual lots. The carbide parameter may also be applicable to conventional fatigue (i.e., bending, rotating-bending, etc.). However, application of the carbide parameter should be confined to either high-speed tool steels or AISI 52100 (L series tool steels).

There appear to be two distinct criteria in the selection of a through-hardened rolling-element material. First, rolling-element fatigue life is a function of material hardness. Second, life is a function of carbide size, area, and number as represented by the carbide factor. These two criteria can be combined to both determine and evaluate without extensive testing the fatigue life of a bearing material or groups of materials.

Combining equations (5), (6) and (7), dropping the subscripts 2 and 3, and letting $L_A = L_3$ where L_A is the expected bearing life at a 90= percent probability of survival

$$L_A = kC'e^{m\left\{[(Rc)_{RT} - 60] - \alpha(T_T - 70)^{\beta}\right\}}\left(\frac{C}{P}\right)^n \qquad (8)$$

where k is a factor which combines processing and environmental factors which can affect bearing life [33]. For AISI 52100 steel $m = 0.1$ [4]. Values of m for other bearing materials have not been experimentally determined. However, they can reasonably be assumed to also equal 0.1. Values for α and β can be obtained from [28-30]. For ball and roller bearings n is equal to 3 and 10/3, respectively.

Ceramics and Cermets

There is a need for bearings to operate reliably at nominal speeds and loads at temperatures to 2000° F. Since the temperature range between 800° and 2000° F is beyond the range in which current ferrous and nonferrous bearing materials are capable of operating, the more refractory materials and compounds must be considered. Among these materials are alumina, titanium carbide cermets, silicon carbide and silicon nitride. A relatively large amount of research and development has been performed with alumina and titanium carbide cermets in rolling-element bearings. Data have also been reported on the use of silicon carbide and silicon nitride.

On the basis of the investigations of [34-36] present-day ceramic fabrication techniques appear to be unable to supply high-quality material for rolling elements for high-temperature applications. As ceramic

materials approach homogeneity and zero porosity, however, high-temperature bearing reliability and load capacity should improve.

Surface failure tests in rolling contact were conducted in the five-ball fatigue tester with both hot-pressed and cold-pressed alumina balls [34,35]. The major impurities present in the 99-percent pure alumina were magnesium, silicon, and iron, which produced a complex spinel phase with a lattice parameter similar to that of nickel aluminate. This material contained about 0.6 volume percent pores; its surface finish was 0.3- to 0.5-μin. rms. The dynamic load carrying capacity at room temperature was found to be 7 percent that of AISI M-1. At 2000° F the dynamic load capacity of alumina was approximately 2 percent that of AISI M-1 at room temperature.

The balls made of the 99-percent pure, cold-pressed-and-sintered alumina material were not found to be of uniform composition. Further examination of these balls indicated that the surface of the as-received specimens showed a roughness of from 3- to 8-μin. rms. This relatively poor surface was the result of 4.3 volume percent pores in the material. The cold-pressed alumina exhibited dynamic load capacity of 15 percent that of the hot-pressed alumina or approximately 1 percent that of AISI M-1 bearing steel [34, 35].

Self-bonded silicon carbide contains approximately 12 volume percent of silicon which is relatively soft and has a low modulus of elasticity. Unlubricated rolling-element tests of this material [37] indicated minimal wear relative to other materials reported at a maximum Hertz stress of 375 000 psi for over 250 million stress cycles of operation. Macroscopic

examination of the running track revealed no surface cracking or spalling.

At 80° F in the five-ball fatigue tester this material had a dynamic load capacity of approximately 1 percent that of AISI M-1 steel [35, 36]. Preliminary tests with molybdenum disulfide-argon mist lubrication at a maximum Hertz stress of 400 000 psi show that self-bonded silicon carbide exhibits excessive plastic deformation at temperatures as low as 1600° F. This would indicate that this material is limited to less severe conditions of temperature and stress.

In [38] the data indicated that a 20-mm bore, titanium carbide cermet ball bearing was capable of running to temperatures of 1200° F for periods of 2 to 3 hours at DN values of approximately 1/2 million with a solid-film lubricant.

Work was reported in [39] with a bearing with titanium carbide races and alumina balls run at moderate loads with molybdenum disulfide lubricant carried in an inert gas. The bearings operated at temperatures to 1500° F for periods as long as 8 hours. Failure of these bearings was by pitting of the titanium carbide races. However, tests performed in the five-ball fatigue tester [35, 36] with a nickel-bonded titanium carbide cermet at a maximum Hertz stress of 310 000 psi at temperatures as low as 1100° F indicated excessive plastic deformation of the material. This result would tend to indicate that the nickel-bonded titanium carbide is limited to a less severe condition of temperature and stress.

The surface failures in titanium carbide very closely resembled those in alumina. Because of the lack of porosity, the relatively small number

of surface pores, and the presence of the ductile matrix, the failure mechanism in this material would not be expected to be the same as that in alumina (i.e., brittle fracture). (The nickel-titanium carbide cermet involves a ductile nickel matrix in which 71 volume percent of fine, evenly divided carbide particles are uniformly dispersed.) Brittle fracture may have occurred, however, in the carbide particles because of the high volume fraction of this phase present. The dynamic load capacity of this material at room temperature was approximately 3 percent of AISI M-1 steel.

Hot-pressed silicon nitride is a ceramic material which has been proposed for rolling-element bearings as well as for journal bearings [40].

Hot-pressed silicon nitride 12.7 mm (0.500 in.) diameter balls were fabricated from one batch of material [41]. The balls were made from cubes cut from silicon nitride plate material and were finished to a AFBMA grade 10 specification. Surface finish of the balls was 2.5 to 5.0×10^{-6} cm (1 to 2 μin.) rms. The five-ball fatigue tester was used to test the balls at a maximum Hertz stress of 5.52×10^{9} N/m^2 (800 000 psi) at a race temperature of 328 K (130° F). The ten-percent fatigue life of the silicon nitride balls was approximately one-eighth of that of the AISI 52100 balls and approximately one-fifth that of the AISI M-50 balls [41].

The spalls on the silicon nitride balls are similar in appearance to those in bearing steels except that those on the silicon-nitride balls were slightly smaller. The spall depth was similar to those on steel balls, unlike those on aluminum oxide and silicon carbide balls which were much shallower. No measurable wear was detected on any of the silicon nitride test balls [41].

On the basis of load capacity (the contact load in pounds that will produce failure of ten-percent of a group of test balls in one million stress cycles), the silicon nitride balls were compared with the AISI 52100 and AISI M-50 data. The capacity of the silicon nitride is only about one-third that of the two typical high quality bearing steels. In comparing these results with those obtained with the other ceramic materials, the silicon nitride appears to be superior to materials such as aluminum oxide, silicon carbide, and titanium carbide for rolling-element bearing applications.

PROCESSING VARIABLES

Component Hardnesses

The effect of component hardness combinations on the fatigue life of SAE 52100 rolling elements subjected to repeated stresses applied in rolling contact was studied in the five-ball fatigue tester [42, 43]. Groups of upper test balls (analogous to the inner race of a bearing) with nominal Rockwell C hardnesses of 60, 63 and 65 were run against lower test balls (analogous to the balls of a bearing) of nominal Rockwell C hardnesses of 60, 62, 63, 65 and 66. These results indicated that, for a specific upper test ball (race) hardness, the rolling-element fatigue life and load-carrying capacity of the test system increased with increasing lower test ball hardness to an intermediate hardness value where a peak life was attained. The peak life-hardness combination occurred for each of the three lots of upper test balls (races) in which the hardness of the lower test balls was approximately 1 to 2 points Rockwell C greater than that of the upper test ball (race). According to these results, for

SAE 52100 steel, a maximum bearing fatigue life should occur when the balls of the bearing are 1 to 2 points harder than the races.

Rolling-element fatigue tests were then performed on AISI 52100 207-size deep-groove ball bearings with inner and outer races from the same heat of air-melt material a nominal Rockwell C hardness of 63 and balls from a second heat of air-melt material tempered to nominal Rockwell C hardnesses of 60, 63, 65 and 66 [43, 44]. Subsequent to testing, the bearings were regrouped according to their actual values of ΔH for Rockwell C hardness increments of 0.5 and 1.0, where ΔH is the difference between the actual hardness of the rolling elements in the bearing and the actual hardness of the inner race. The results of these tests are shown in Fig. 11. Other bearing data taken from [45] were reanalyzed and plotted in Fig. 12. Both sets of bearing data exhibited a maximum life for a ΔH of approximately 1 to 2 points Rockwell C. These results correlated with those obtained with the five-ball fatigue tester.

Current state-of-the-art heat treat quality control of bearing components causes significant hardness variation for any given hardness specified. As an example, bearings in any single group of commercial bearings can have a ΔH spread of over 6 points Rockwell C. By using various hardness tolerances for races and balls, theoretical ΔH ranges for specified ΔH were determined. These data indicate that the benefits derived from ΔH are a function of hardness control and proper matching of balls and races. Where care is not taken to properly match balls and races, no improvement in fatigue life would be expected by specifying ΔH [43].

Controlled Fiber

A technique which has been used to improve bearing life is the manipulation of the material fiber orientation. The races and rolling elements of most bearings are forged. Any metallic object formed by forging generally possesses a fiber-flow pattern which reflects the flow of metal during the forging operation. Carbides and nonmetallic inclusions are progressively and directionally oriented during each forming operation from the ingot to the final bearing-element shape. Although the desired microstructure is obtained by heat treatment, the carbides and inclusions generally retain their processing-induced directionality. This pattern is fibrous in appearance when the part is macro-etched, hence the term "fiber-flow lines." In addition, the entire grain pattern is preferentially oriented in the same manner.

The type of forging used to produce rolling-element bearing components will determine the fiber pattern which exists in these bearing parts. Steel balls are usually fabricated by upsetting between hemispherical dies. This fabrication technique produces a fiber-flow pattern with two diametrically opposed areas having fibers oriented approximately perpendicular to the surface as illustrated in Fig. 13. These areas are commonly known as the poles. The excess metal extruded from between the two dies produces a thin band of perpendicularly oriented fiber when the flashing at the die parting line is removed. This line, when present, is commonly termed the "equator". Thus, a typical ball has several surface areas with varying fiber-orientation. The initial effect of fiber orientation on fatigue life was reported in [17, 18]. Two lots of AISI 52100 balls were modified

during manufacture to predetermine the axis of rotation and to enable one lot to be run over the poles and the other lot over the equator. The results obtained indicated a significant improvement in fatigue life when the test track passed over areas other than the poles.

Fatigue data obtained with ten different ball materials was also examined with respect to the location of specific spalls on the ball test specimens. Each of the ball specimens was destructively etched after the test to indicate the location of the failure relative to the pole areas. These data showed that a small increase in failure density occurs at the equator where the thin band of perpendicular fiber exists and that a very significant increase in failure density occurred in the polar areas or regions where fiber is essentially perpendicular to the test surface.

Attempts were made to control fiber flow in balls [46], but these were either unsuccessful or did not produce any significant improvement in fatigue life.

While the feasibility of controlling fiber flow in balls is questionable, the opposite appears to be true in bearing races. Additional research [4] with controlled fiber flow was performed by machining race cylinders from a billet of AISI T-1 steel at various angles to the direction of forging as illustrated in Fig. 14. Three cylinders (races) were machined with axes parallel to, at 45° to, and perpendicular to the direction of fiber flow. The first cylinder (race) had fiber flow parallel to the test surface, the second had fiber orientation ranging continuously from parallel to 45° to the test surface, and the third had fiber orientation ranging continuously from parallel to perpendicular to the test surface. The 0°

cylinder (race) had the best life while the 0° to 45° and the 0° to 90° cylinder (race) indicated that five of the six lowest lived failures occurred in the 81° to 90° zone. The ten-percent life (the life at a 90-percent probability of survival) for perpendicular fiber was found to be about 1.25 million stress cycles as compared with 4.7 million stress cycles for parallel fiber.

Experiments confirming the results of [17, 18] were reported in [47]. Bearings were manufactured by two methods [47] as shown in Figs. 15 and 16. One method produced races with conventional fiber orientation (Fig. 15). The other method incorporated forging techniques which produced parallel fiber flow (Fig. 16). Fatigue results from these two methods show at least a ten fold increase in life of the bearings having side grain or fiber flow parallel to the race as opposed to bearings made with the end grain races or fiber nearly perpendicular to the running track. It was also determined that the same heats of steel which gave poor life when forged with enddgrain in the race performed very creditably when forged with side grain in the race. The life of parts seemed less sensitive to steel quality variations when forged with the fiber flow parallel to the race.

If bearings with side grain (parallel fiber flow) were radially loaded, no difference in life would be expected between these bearings and those conventionally forged. The reason for these results is that the conventionally forged bearing will generally produce parallel fiber flow in the portion of the race groove which is subject to the radial load.

Ausforging

Within recent years a thermo-mechanical process termed "ausforging"

has been evaluated which has shown great potential in improving bearing fatigue life. The term "ausforging," "ausformed," and the like, are used to describe processing techniques which consist of the working of a steel while the material is in the metastable austentic condition.

Ausforging has been studied since 1954 [48]. Since then a number of organizations both in the U.S. [49-51] and abroad [52] have investigated the process. The application of ausforming to rolling-element bearings was first performed in 1965 [5]. The material used in this work was AISI M-50 because this alloy has the required metallurgical transformation characteristics for ausforming, as illustrated in Figs. 17 and 18. Fig. 17 is the transformation diagram for AISI 52100. In this material the phase changes occur rapidly upon quenching from the austenite range, and there is not sufficient time to effect any type of deformation in the austenite prior to its transformation to martensite. Fig. 18 illustrates the transformation behavior of an AISI M type tool steel where the austenite is isothermally stable for a sufficient length of time to work the material.

Initial rolling-element fatigue tests were performed with cylindrical rollers made from ausformed AISI M-50 material having 40, 70, and 80 percent deformation [5]. The results of these tests are shown in Fig. 19. It can be seen that the ausformed material is superior to the normally processed AISI M-50. Additionally, a relation exists between the amount of deformation during ausforming and fatigue life. Tests with ausformed AISI M-50, 35-mm bore, single-row radial ball bearings [53] having 80-percent deformation produced fatigue lives approximately eight times conventionally forged AISI M-50 bearings.

Ausformed balls were fabricated from M-50 bar material which was extruded to a cross-sectional area 20 percent of the original area (80 percent reduction in cross-sectional area) while the material was in a metastable austenitic condition. The 10-percent fatigue life of this group of ausformed balls was three and four times that of two groups of conventionally processed M-50 balls [54].

It is believed that the primary mechanism causing the improved fatigue life is "strain induced precipitation". In essence, sufficient energy is imparted to the material during ausforming which results in precipitation of the carbides in the material. This results in smaller and more uniformly dispersed carbides because of the availability of a larger amount of carbide nucleation sites during the ausforming process [5].

Residual Stresses

An analysis presented in [55] indicates that a compressive residual stress that exists at the depth of the maximum shearing stress can decrease the maximum shearing stress. A similar analysis for superimposed stresses was subsequently reported in [56] and [57]. Although observations [58] would indicate that the maximum orthogonal shearing stress is the critical stress in the initiation of fatigue cracks, there also is evidence [4, 19, 59, 60] that the maximum shearing stress is the most significant stress in the fatigue process. Thus, if the maximum shearing stress for a given Hertz stress could be decreased by compressive residual stresses, rolling-element fatigue life could be increased [55].

Residual stress can either increase or decrease the maximum shearing stress according to the following equation:

$$(\tau_{max})_r = -\tau_{max} - \frac{1}{2}(\pm S_r) \qquad (9)$$

where τ_{max} is the maximum shearing stress, $(\tau_{max})_r$ is the maximum shearing stress modified by the residual stress, and S_r is the residual stress, the positive or negative sign indicating a tensile or compressive residual stress, respectively [55]. Accordingly, a compressive residual stress would reduce the maximum shearing stress and increase fatigue life according to the inverse relation of life and stress to the 9th power where

$$L \propto \left[\frac{1}{(\tau_{max})_r}\right]^9 \qquad (10)$$

Compressive residual stresses induced beneath the surface of ball-bearing race grooves were found beneficial to rolling-element fatigue life [61 and 62]. Ball bearing lives were increased by a factor of 2 when metallurgically induced ("prenitrided") compressive residual stress was present in the inner rings (group B, Fig. 20) [61]. Compressive residual stresses induced by unidentified "mechanical processing" operations were also found to be beneficial to the fatigue life of ball bearings [62].

Compressive residual stresses can be induced as a result of the cyclic concentrated contact in rolling-element bearings [59, 63-66]. These stresses depend on plastic deformation of the microstructure. They tend to reach a maximum at a depth of several mils beneath the rolling surface corresponding approximately to either the depth of the maximum shearing stress [56, 65, 66] or the depth of the maximum orthogonal shearing stress [59]. The magnitude of the residual stress tangential to the surface in the direction of rolling is dependent on both the applied load and the number

of load cycles. Research reported in [45] indicates a threshold load below which significant residual stresses are not induced except for very long running times.

Changes in microstructure (phase transformations) have been reported to occur in the same areas as the maximum induced residual stress [45, 65]. Under some conditions of very high contact stresses, no microstructural alteration was apparent where significant residual stresses were induced in a few cycles [45]. The correlation of induced residual stress with these microstructural alterations is not clear. In [66], they are proposed to be independent phenomena.

It was reported in [59] that there were significant effects of residual stress induced during fatigue testing on rolling-element fatigue life. In this work, maximum compressive residual stresses were induced and maximum fatigue life resulted when the ball hardness was 1 to 2 points Rockwell C greater than the race hardness (ΔH = 1 to 2 points Rockwell C). An identical effect is reported in [66].

It was hypothesized that such a beneficial compressive residual stress could be induced by prestressing a ball-bearing inner race; for example, by running the bearing at a load greater than the threshold load [63] for a prescribed number of cycles. The bearing, when subsequently run under more nominal service loads, would then be expected to experience a longer fatigue life. Twenty-seven bearings were subjected to this prestress cycle and subsequently fatigue tested at a radial load which resulted in a maximum Hertz stress at the inner- race - ball contact of 2.4×10^9 N/m^2 (350 000 psi) [67]. The results of these tests were compared with results

of baseline tests without a prestress cycle at identical test conditions. The 10-percent fatigue life of the prestressed ball bearings was greater than twice that of the baseline bearings. Additionally, it was determined that differences between the measured residual stress in the prestressed bearings and in the baseline bearings after 3000 to 4000 hours of testing are small [67].

OPERATING VARIABLES

Speed Effects

The basic load ratings [69], which are based on a concept originally developed by Lundberg and Palmgren [31, 48, 68], may be used to predict bearing life when the load is not excessive, the speed is moderate, and the bearing is effectively lubricated. The rating life is calculated from Equation (3). Life in hours, is commonly assumed to be inversely proportional to the speed of operation and is calculated by dividing Equation (3) by the revolutions per hour in the application. At high speeds, however, the load distribution on the rolling elements and the zone of loading may change because centrifugal growth and differential thermal expansion between the rings can change the bearing operating clearance. In addition to the redistributed loading, centrifugal force from the orbiting rolling elements augments the loading at the outer raceway and tends to reduce fatigue life below that predicted by the standard. High-speed operation shortens the fatigue life of the outer raceway because of centrifugal loading, which increases as the square of the rolling-element orbital speed.

Fig. 21 shows the effect of centrifugal load on the life calculations for a 20-mm bore radial ball bearing, operating under a 100-lb radial load (5 percent of the dynamic load capacity, C) and having a nominal zero radial clearance. The dynamic load capacity C is defined as the load the bearing can carry for one million inner ring revolutions with a 90 percent probability of survival. The divergence between the standard life and the high-speed life with increasing speed also illustrates the increasing importance of centrifugal load, as a percentage of the application load, in determining the fatigue life of the bearing.

As the external radial load increases, the difference between fatigue lives calculated by conventional means and those calculated by taking into account high-speed effects decreases. Fig. 22 illustrates this effect. The data from Fig. 21 is replotted on Fig. 22 as the ratio of the fatigue lives calculated by the Lundberg-Palmgren method [58] with and without centrifugal force effect, versus the speed parameter DN. For comparison purposes, a similar plot was constructed for a 300-lb radial load (15 percent C). At higher speeds, errors are introduced into conventional life calculations by neglecting centrifugal load increases with speed and with reduction in the applied load. Because of the increased loading of the outer race at high speeds, the relative probabilities of fatigue failure in the races changes, and the bearing life is different from that calculated by the Lundberg-Palmgren formula [70].

Digital computer programs that can evaluate these effects simultaneously are extremely valuable tools in reducing the time and expense of laborious

hand calculations to determine the rolling-element loadings to be used in estimating bearing life [70].

Preliminary bearing endurance tests [25] were conducted with the 24° contact-angle bearing at a speed of 25 000 rpm (3 million DN) and a thrust load of 22241 N (5000 lb). Under these conditions the maximum Hertz stresses in the inner and outer races are 1965×10^6 and 2096×10^6 N/m^2 (285 000 and 304 000 psi), respectively. The standard life calculation [70] predicts a bearing 10-percent life under these operating conditions of approximately 16 hours considering centrifugal force effects. However, using the material, lubricant and speed factors given in [33], a 10-percent life of about 175 hours would be a more reasonable prediction. Of the ten bearings initially tested all ran for 1000 hours without failure. These results [25] show that, in spite of centrifugal effects, long-term bearing operation at 3 million DN can be achieved with a high degree of reliability using sophisticated but currently available state-of-the-art bearing materials and designs, lubricants, and lubrication techniques.

Temperature Effects

A problem which exists in high-temperature turbine engines is the high-ambient temperature to which the engine and its components will be exposed. Bearing temperatures can range between 400° and 600° F (478 and 588 K) in present and advanced engine designs.

Research reported in [71-74] indicates that a synthetic paraffinic oil can give lives in excess of AFBMA-predicted (catalog) life at a temperature of 600° F (588 K) under a low-oxygen environment (less than 0.1 percent oxygen by volume).

The bearing operating temperature will affect both the bearing steel and the lubricant. As bearing temperature is increased the hot hardness of the bearing steel decreases. Research reported in [7 and 8] indicates that a one point Rockwell C hardness increase may mean a two-fold increase in bearing fatigue life. Conversely, a decrease in room-temperature hardness can conceivably decrease bearing life.

When considering rolling-element fatigue, viscosity is probably the most important single property of a liquid lubricant. For a given lubricant, viscosity is a function of temperature. As temperatures are increased, the viscosity of the fluid is decreased. The decrease in viscosity affects both the bearing fatigue life and the elastohydrodynamic (EHD) film thickness which separates the mating surfaces in a bearing.

Investigators have shown [4 and 5] that, as the viscosity of a mineral oil lubricant is increased, rolling-element fatigue life also increased. The accepted relation between life L and lubricant kinematic viscosity ν is

$$L \propto \nu^{n} \tag{11}$$

where $n = 0.2$ or 0.3.

In order to assure proper bearing operation a lubricant film, termed an elastohydrodynamic film, is required to separate the contacting components. From elastohydrodynamic theory [76], the accepted relation between film thickness H and viscosity is

$$H \propto \nu^{0.7} \tag{12}$$

Equating equations (11) and (12) and using a value of $n = 0.25$

$$L \propto H^{0.36} \tag{13}$$

While the EHD and material hardness effects are independent of each other, they are both directly dependent on temperature. As temperature increases both effects act toward decreasing life. Combining equations (5) and (13),

$$L \propto H^{0.36} \cdot e^{m\left\{[(Rc)_{RT} - 60] - \alpha(T_T - 70)^{\beta}\right\}} \qquad (14)$$

Groups of 120-mm bore angular-contact ball bearings made from AISI M-50 steel were fatigue tested with a synthetic paraffinic oil at bearing temperatures of 400°, 500°, and 600° F (478, 533, and 588 K) [27]. Relative life results for these bearings were calculated using equation (14). The relative experimental and predicted lives are presented in Table I. These results indicate reasonably good agreement between the experimental and predicted lives. The most important result of these tests was that under adequate EHD lubrication the differences in lives between 478 and 588 K (400° and 600° F) were statistically insignificant [27].

DESIGN OPTIMIZATION

Internal Geometry

Rolling-element bearings are being exposed to increasingly severe operating conditions coupled with stringent fatigue life requirements and, frequently, severe limitations on the rate of heat absorption by the lubrication system. It is extremely important, therefore, to achieve optimum bearing designs in terms of either maximum fatigue life or minimum heat generation. A considerable analytical effort has therefore been expended to develop a better understanding of rolling-element bearings, in general, and of angular contact ball bearings, in particular.

An accurate prediction of the operatin g characteristics of a high speed angular-contact ball bearing is a formidable task because the complete force system acting on the balls must be known. The principal difficulties lie in accurately characterizing cage forces and the elastohydrodynamic pressure and tractive forces in the ball-race contacts. The initial analyses of ball bearing dynamics, such as [77], were made before much work had been published on elastohydrodynamics. Therefore, coulomb friction was assumed to exist in the ball-race contacts; this led to the raceway-control theory of ball-bearing operation. The gradual development of elastohydrodynamic theory made it apparent that the assumption of coulomb friction is not reaslistic in a rolling-element bearing lubricated with copious quantities of oil [78].

The first analysis which incorporated elastohydrodynamic forces into ball dynamics was presented in [79]. This analysis resulted in better prediction of ball skidding at high speeds and light loads, although simple linear shear, an exponential model for the lubricant pressure-viscosity, and Newtonian behavior of the oil were assumed in calculating tractive forces. In [80] it was found that the assumption of a Newtonian fluid with an exponential pressure-viscosity relationship gave impossibly high values of torque. A more reaslistic type of model was developed in [80] and this has been incorporated into the ball bearing analysis of [81]. Considerable work needs to be done to more accurately define lubricant rheological behavior in the Hertzian contacts of high-speed, rolling-element bearings.

The dynamic analyses [77, 79, 81] have proven invaluable in optimizing

bearing internal geometry for maximum fatigue life, and in assessing the effects of speed on life. When ball bearings are operated at DN values above 1.5 million, centrifugal forces produced by the balls can become significant. The resulting increase in Hertz stresses at the outer-race ball contacts may seriously shorten bearing fatigue life. It is therefore logical to consider methods for reducing the factors that contribute to ball centrifugal loading, such as ball mass, ball orbital speed, and orbital radius. Theory indicates that reductions in ball mass can be quite effective in extending bearing fatigue life at high speeds [81].

Cages

Cages are a much more severe problem in small bore bearings than in larger ones. In extreme-speed applications of small bore bearings, it is frequently necessary to use a silver-plated, semi-hard, tool-steel retainer rather than a bronze, and oil-mist lubrication rather than re-circulating oil to reduce churning losses. In large bore bearings, retainer failure is much less common than in small bore bearings [82].

At temperatures above 500° F, tests have indicated that bearing cage wear can be a limiting factor in the operation of bearings under the severe lubrication conditions encountered at these elevated temperatures. Therefore, in addition to the race and the rolling-element material, careful consideration must be given to the choice of cage material.

In conventional rolling-element bearings, both metallic and non-metallic cages have found widespread use. Under normal temperatures, for nonaerospace applications, practically all the roller bearings and a large percentage of the ball bearings in use have been equipped either with

stamped cages of low-carbon steel or with machined cages of iron-silicon bronze or lead brass. Precision bearings, such as those used for aerospace applications, are usually equipped with cages machined from copper alloys or nonmetallic phenolic materials. In some applications, where marginal lubrication exists during operation, such as at high temperatures, silver plating on the bronze has been used. Phenolic materials are limited to temperatures of approximately 275° F, while copper-base alloys are suitable for operation to approximately 600° F. Above 600° F, some success has been obtained with low-carbon steel or cast-iron cages, but, generally, the most successful high-temperature cages have been nickel-base alloys. One of the nickel-base alloys used was AMS 4392 (S-Monel). Other materials which have shown promise are high-temperature plastics which exhibit low friction and wear characteristics, high-alloy steels capable of maintaining their hot hardness at elevated temperatures, and stainless steels.

In general, potential high-temperature cage materials of the types reported herein should be heat-treated to their maximum room-temperature hardness, while sufficient ductility to prevent cracking is maintained. In application, however, the rolling-element material should be somewhat harder than the cage material to prevent damage to the rolling elements. Wear-resistant platings or coatings may also be used to reduce cage wear [82].

Cages for ball bearings may be piloted on the inner or outer ring or on the balls. In cylindrical roller bearings, the cage may be piloted on either the inner or outer ring or on the rollers. Ball and roller piloted cages are speed limited and seldom find use in high speed bearings.

Of necessity they are two piece, stamped or machined, bolted assemblies. One piece cages have a distinct advantage for high-speed applications. They are easily balanced and they are structurally stronger than two piece cages.

The advantages of inner- and outer-ring piloting have long been argued. An outer-ring piloted cage is self-balancing (it wears itself into balance) and the cage piloting surface is easier to lubricate at high speeds because centrifugal effects assist in getting oil to this critical location. On the other hand, outer-ring piloted cages are sensitive to dirt ingestion. Wear of the outer-ring and cage usually results in applications where the lubricant cannot be kept clean.

In contrast, inner-ring piloted cages wear themselves out of balance, and the piloting surface is difficult to lubricate at high speeds with simple jet lubrication. They are much less sensitive to dirt, however, and direct lubrication of the cage piloting surface (discussed in the section LUBRICATION METHODS) has alleviated the cage wear problem at high speeds. Experience indicates that bearings with inner ring piloted cages operate at somewhat lower temperatures.

POWER LOSS

Power loss in rolling-element bearings is difficult to predict because of the complexity of bearing dynamics and lubricant rheology, and because of its extreme sensitivity to the mode of lubrication. Early attempts to develop formulae for the calculation of power losses in bearings were not practical because of the many coefficients that had to be determined experimentally. More recent work [83, 84] has concentrated on the development

of an analytical model, based on previously developed spinning friction models, which includes rolling and spinning under lubrication regimes from thin film to flooded conditions.

LUBRICANT EFFECTS

Application of Elastohydrodynamics

As previously mentioned, the film formed between nonconforming bodies in Hertzian contact as a result of the elastic deformation of the material and the hydrodynamic action of the lubricant is called an elastohydrodynamic film. This film, which is generally dependent on lubricant base stock and viscosity, is in the order of 5 to 10 millionths of an inch thick at elevated temperatures [85].

When a sufficient EHD film is present, rolling-element bearings will not usually be subjected to early failures as a result of surface distress. They will fail from rolling-element fatigue. Fatigue usually manifests itself, in the early stages, as a shallow spall with a diameter about the same as the contact width. A typical fatigue spall of a bearing inner race is shown in Fig. 4.

As atmospheric viscosity of a particular lubricant is increased, rolling-element bearing fatigue life also increases. If the lubricant pressure-viscosity coefficient is increased by changing the lubricant base stock, longer fatigue life can be obtained for a given lubricant at atmospheric conditions. It has become generally accepted that fatigue life increases with increases in viscosity, pressure-viscosity coefficient, or rotational speed. These factors imply increasing bearing fatigue life with increasing EHD film thickness.

The importance of maintaining a sufficient elastohydrodynamic (EHD) film thickness between dynamically contacting machine elements has in recent years been more fully appreciated. The prediction of EHD film thickness has been the focal point of many theoretical and experimental investigations, and has been summarized well in [76, 86].

A lubricant film parameter Λ has become an acceptable indicator of the effectivness of the lubricant film within the rolling-element contact zone.

$$\Lambda = \frac{h_{min}}{\sigma} \tag{15}$$

where

h_{min} minimum film thickness, m (in.)

σ surface composite roughness $[\sigma_1^2 + \sigma_2^2]^{1/2}$, rms, m (in.)

σ_1, σ_2 surface finish of elements 1 and 2, rms, m (in.)

It has been shown that Λ influences the fatigue life of rolling-element bearings (Fig. 23) [87-89]. Predetermination of this lubricant parameter with an accurate prediction of minimum film thickness will be of value to the designer in obtaining more realistic estimates of rolling-element fatigue life [33].

The bulk of the experimental work conducted in elastohydrodynamic lubrication has been confined to conditions of moderate speeds; that is, up to 25.4 meters per second (1000 in./sec), and moderate loads; that is, maximum Hertz stresses to 1.24×10^9 N/m^2 (180 000 psi) [90-93]. The research of [94, 95] has extended the EHD film thickness measurements to maximum Hertz stresses of 2.42×10^9 N/m^2 (350 000 psi) which include the design operating range of most machine components such as bearings and gears.

This data was obtained on a rolling-disk machine using an X-ray transmission technique to measure minimum film thickness. The film thickness measurements showed good qualitative agreement with full-scale bearing test results [27]. That is, very low film thicknesses were measured at conditions similar to those where the bearings suffered surface damage.

In contrast to the results obtained by previous investigators which showed reasonably good correlation at moderate speeds and loads between elastohydrodynamic theory and film thickness measurement, the data of [94, 95] showed a marked deviation between predicted and experimental values of film thickness. In particular, at high contact stresses; that is, maximum Hertz stresses greater than 1.38×10^9 N/m^2 (200 000 psi), the sensitivity of the film thickness to load as determined experimentally is far greater than that predicted by classical EHD theory of [96, 97].

Several attempts have been made to resolve the apparent discrepancy between theory and experiment. A critical examination of the X-ray technique itself was made [98] for possible load dependent experimental errors. However, no experimental factors were uncovered which could seriously alter the accuracy of the X-ray measurements. On the theoretical side, the influence of several possible rheological factors has been investigated, such as the effects of a non-Newtonian lubricant of the Ree-Eyring form [99], the effects of heating at the inlet of the contact region [100], and the effects of a reduced lubricant viscosity-pressure dependence using a composite exponential model [101] and using a power-law model [102].

While each of the above modifications to elastohydrodynamic theory has succeeded somewhat in improving the agreement between theory and

experimental data within the heavy load regime, the resulting predicted values of film thickness differed little in magnitude from those computed using classical EHD theory. Furthermore, the modified theories do not sufficiently account for the high film thickness-load dependence to allow accurate predictions of film thickness under realistic operating conditions.

The experimental data of [100, 101] also show a film thickness sensitivity to stress greater than theoretical for maximum Hertz stresses greater than about 1.04×10^9 N/m^2 (150,000 psi). These data, obtained by an optical interferometry technique with sliding point contacts tend to confirm the measurements obtained by the X-ray technique of [94, 95].

The isothermal theory of Cheng [103] is considered representative of those EHD theories which predict nominal film thickness for bodies in line contact. Cheng's EHD equation can be written

$$\frac{h_c}{R'} = 1.47\left(\frac{\alpha \mu_o u}{R'}\right)^{0.74}\left(\frac{p_{Hz}}{E'}\right)^{-0.22} \tag{16}$$

where

E_1, E_2 modulus of elasticity of elements 1 and 2, N/m^2 (psi)

E' $\left(\frac{1 - \nu_1^2}{\pi E_1} + \frac{1 - \nu_2^2}{\pi E_2}\right)^{-1}$ N/m^2 (psi)

h_c film thickness in Cheng's theory, m (in.)

pH_z maximum Hertz stress, N/m^2 (psi)

R' equivalent radius, $\left(\frac{1}{R_1} + \frac{1}{R_2}\right)^{-1}$, m(in.)

R_1, R_2 radius of elements 1 and 2 in rolling direction, m (in.)

mean surface velocity, $1/2(u_1 + u_2)$, m/sec (in./sec)

u_1, u_2 surface velocities of elements 1 and 2, m/sec (in./sec)

α pressure-viscosity coefficient, m^2/N (psi^{-1})

μ_o inlet absolute viscosity, N-sec/m^2, (lb-sec/$in.^2$)

$\nu_{1,2}$ Poisson's ratio of elements 1 and 2

An empirical elastohydrodynamic (EHD) film thickness formula for predicting the minimum film thickness occurring within heavily loaded contacts (maximum Hertz stresses above 1.04×10^9 N/m^2 (150 000 psi)) was developed and reported in [104]. The formula was based upon X-ray film thickness measurements made with synthetic paraffinic, fluorocarbon, Type II ester and polyphenyl ether fluids covering a wide range of test conditions. This formula can be written as follows:

$$\bar{H}_{min} = K_j \bar{U}^{0.62} \bar{P}_{Hz}^{-0.22} \phi_s \qquad (17)$$

where

$\bar{H}_{min}$ nondimensional minimum film thickness, $\frac{h_{min}}{R'}$

h_{min} minimum film thickness, m (in.)

j test lubricant subscript

K_j lubricant coefficients in empirical film thickness formula

$\bar{P}_{Hz}$ nondimensional stress parameter, p_{Hz}/E'

$\bar{U}$ nondimensional speed-viscosity parameter, $\mu_o u/E'R'$

ϕ_s high contact stress factor

A comparison between standard EHD theory [103] and the empirical EHD film thickness formula [104] is presented in Fig. 24. The deduced relation-

ship adequately reflects the high-load dependence exhibited by the measured data.

Additives

Lubricant additives can prevent or minimize wear and surface damage to bearings and gears whose components are in contact under very thin film or boundary lubrication conditions. These antiwear or extreme pressure (EP) additives either adsorb onto the surfaces or react with the surfaces to form protective coatings or surface films. The value of additives for this protection is well known, and their use is commonplace.

In rolling-element bearings, these additives aid in protecting the rubbing contacts between the cage and the balls or rollers and between the cage and the race guiding lands. Also, it has been shown [71] that antiwear additives can protect the ball-race contacts in ball bearings operating under high-temperature high-speed conditions where lubrication conditions are marginal. In the tests of [71], gross surface distress and wear were eliminated with the addition of a low concentration of a substituted organic phosphate antiwear additive to a synthetic paraffinic lubricant. Further work [94] confirmed that significant surface films are generated under similar high-temperature, high-speed conditions. These surface films produced an apparent increase in the elastohydrodynamic (EHD) film thickness between rolling disks as measured by the X-ray transmission technique.

The effects of lubricant antiwear and EP additives on rolling-element fatigue life are not well defined. When a rolling-element bearing is operating under conditions with a full EHD film separating the rolling

elements, little, if any, asperity contact occurs and the life of the bearing is limited only by rolling-element fatigue. If, however, the film thickness is reduced such that significant asperity contact occurs, the life of the bearing is reduced [88, 89]. This life reduction is greater with increased frequency of asperity contact. Under these conditions, classical subsurface initiated rolling-element fatigue becomes a less common mode of failure, and excessive surface distress and smearing can become the predominant mode of failure [87]. Under these extreme conditions, surface active additives may be expected to influence bearing life by preventing some of the surface damage as was demonstrated in [71]. However, under full EHD conditions where subsurface initiated rolling-element fatigue is the criterion of failure, these surface active additives should have no effect on bearing life unless the lubricant rheology is significantly altered by the additive or the presence of the surface films.

In [105], the effects of several surface active additives on several bearing steels were investigated in a rolling four-ball tester. Here it was found that either beneficial or detrimental effects on life are obtained with each of several additives depending on the choice of steel. These tests [105] were run under very severe lubricant film conditions where significant surface film effects would be expected. The limiting life in the majority of these tests was of a surface distress type and not classical rolling-element fatigue.

Rolling-element fatigue tests were conducted with a base oil with and without surface active additives [106]. Three steel ball materials were investigated. The 12.7-millimeter- (0.500-in.-) diameter test balls were

either AISI 52100, AISI M-50, or AISI 1018 steel. The test lubricant was an acid-treated white oil containing either 2.5 percent sulfurized terpene, 1 percent didodecyl phosphite, or 5 percent chlorinated wax. Nine combinations of materials and lubricant additives were tested at test conditions including a maximum Hertz stress of 5.52×10^9 N/m^2 (800 000 psi), a shaft speed of 10 700 rpm, and a race temperature of 340 K (150° F).

In general, it was found that the influence of surface active additives was detrimental to rolling-element fatigue life. The chlorinated-wax additive significantly reduced fatigue life by a factor of 7. Rolling-element surface distress was observed in some of the tests. These results suggest that the rheology of the base oil may have been altered by this additive. The base oil with the 2.5 percent sulfurized terpene additive reduced rolling-element fatigue life by as much as 50 percent. No statistical change in fatigue life occurred with the base oil having the 1 percent didodecyl-phosphite additive. The additives used with the base oil did not change the life ranking of bearing steels in these tests where rolling-element fatigue was of subsurface origin [106].

The NASA spinning torque apparatus was used to conduct tests with AISI 52100 steel 1/2-inch (12.7-mm) diameter balls spun against nonconforming groove specimens with a conformity of 55 percent [107]. The lubricant was a synthetic paraffinic oil to which were added 0.1, 1.0, or 10 volume percent of either an antiwear or extreme-pressure (EP) additive. The additives used were stearic acid, oleic acid, oleyl phosphate, oleyl phosphite, and zinc dithiophosphate. Test conditions included maximum Hertz stresses of 60 000 to 200 000 psi (41×10^7 to 138×10^7 N/m^2), a spinning speed of 1000 rpm,

and room temperature (no heat added). The spinning torques were measured for each test condition.

Under the test conditions elastohydrodynamic lubrication prevailed with no significant surface interaction. The addition of the antiwear or EP additives in various concentrations to the synthetic paraffinic oil did not change the spinning torques over those obtained with the base fluid. The viscoelastic properties of the fluid were not changed by the additives tested [107].

LUBRICATION METHODS

Mist

The advantages of mist or once-through vapor lubrication have long been recognized, and a variety of mist lubricators and lubrication systems are commercially available. When compared to recirculating systems, they offer the advantages of reduced complexity because they eliminate sumps and supply and scavenge pumps, and reduced operating torque. Their disadvantage lies in heat removal. An oil-gas mist obviously does not have the heat removal capability for high flow rate recirculating system so that a mist lubricated bearing will run hotter.

Despite this, mist systems are being considered for use in high temperature applications where the feasibility of using organic lubricants in a recirculating system is questioned because of limitations in their oxidative and thermal stabilities. The extent of lubricant degradation is a function of the availability of oxygen and of the time and the temperature to which the lubricant is exposed. Since thermal and oxidative degradation are functions of time and temperature, the use of a "once-through"

lubrication system may be advantageous in some high-temperature applications. Lubricant degradation could be minimized by exposing the lubricant to the high temperature for the shortest possible time.

Since the lubricant is discarded after one pass in a once-through system, economy of use becomes of paramount importance. Thus, the oil-flow requirements of a bearing must be known before the economic feasibility of a once-through system for a specific application can be evaluated.

Some work has been done to define quantitatively the actual oil-flow requirements of ball bearings. In [108, 109] some data are reported on the relation of running time to failure as a function of the quantity of oil, applied prior to the test, for 30- and 50-millimeter-bore ball bearings. In [109], steady-flow minimum oil requirements were obtained from an analysis of the experimental data; these data were used to estimate quantitatively the required bleed rate of greases. Some data on minimum-oil-flow requirements of 25-millimeter-bore ball bearings at a DN (product of bearing bore in mm and shaft speed in rpm) value of 0.9×10^6 are reported in [110].

In [111, 112] extensive minimum-oil-flow data with 75-millimeter-bore ball bearings are reported for a wide range of temperatures, loads, and DN values with two oils. In [111], a MIL-L-7808 diester oil was used in tests conducted at bearing temperatures to 500° F, DN values of 0.975×10^6, and thrust loads to 3000 pounds. In [112] data obtained with a highly refined naphthenic mineral oil at temperatures to 800° F, DN values to 1.2×10^6, and thrust loads to 3000 pounds are reported. From [111, 112], data are available for a broad range of temperatures and loads for 75-millimeter-bore bearings.

In [113] minimum oil flow tests were conducted with 30-millimeter bore ball bearings. A generalized correlation of the data obtained in [111, 112, and 113] is presented in [113]. This is shown in Fig. 25. The resulting curve of Figure 25 may be expressed by the equation

$$\log \frac{Q}{PN} = -51.982 + 0.852 \log PN^5T^8D^3$$

Nomenclature are given in Figure 25. The individual data points are scattered so that, at specific values of the abscissa variable they range from a minimum of $\frac{1}{3}$ to a maximum of $3\frac{1}{2}$ times the flow indicated by the best fit line. These flow ratios, however, are not much greater than the flow intervals used to determine the minimum required oil flows in individual tests.

If values of P, D, N, and T are known, the value of the abscissa variable $PN^5T^8D^3x10^{-48}$ can be calculated. From the best fit line the value of the ordinate variable $(Q/PN)x10^{10}$ can be determined so that Q can be calculated.

More recent work on mist lubrication, such as [114], has concentrated on fundamental wettability studies aimed at producing more efficient mist generators and reclassifying nozzles.

Recirculating Jet

Recirculating jet or nozzle oil systems require more complex hardware than do mist systems (pumps, sumps and heat exchangers) with the consequent weight penalty, but their use in many applications is necessary to maintain thermal equilibrium in the bearings. In high-speed, highly-loaded bearings, mist flow requirements make them uneconomical even when thermal equilibrium can be maintained [113].

There have been many studies conducted to determine optimum jet arrangements. Typical of these is [115] in which the efficiency of single, multiple and multiple opposed jet arrangements was studied.

The effects of oil-air mist and recirculating oil-jet lubrication on bearing operating temperature and torque are illustrated in Figure 26 [116]. The data of Figure 26 were obtained with 75 mm bore conventional ball bearings (solid balls) and with drilled ball bearings. For the conventional bearing at 20 000 rpm (1.5 million DN), the outer race temperature was 250° F with recirculating oil jet lubrication and 345° F with oil-air mist lubrication. The torque, however, was 11.5 in. lbs with oil-jet lubrication and only 3.5 in. lbs with oil-air-mist lubrication.

More recent work has shown that, even with optimum jet arrangements, there is a definite limiting DN value above which a jet system is no longer adequate. Centrifugal effects prevent the oil jets from properly lubricating and cooling the critical bearing internal surfaces. Cage wear or bearing thermal instability results. With fairly large bore ball bearings (on the order of 125 to 150 mm) this limiting DN value occurs at about 2.5 million.

Underrace Lubrication

To overcome the detrimental centrifugal effects in extreme speed applications, oil is introduced directly to the interior of the bearing through radially directed passageways. A typical arrangement for a split inner ring ball bearing, taken from [117], is shown in Fig. 27. Lubricant from the external reservoir was directed by a fixed nozzle into an annular scoop which rotated with the bearing shaft assembly. The lubricant then flowed from the scoop through axially oriented passages in the hub assembly

to radial passages terminating at the bearing bore. Lubricant discharged from the test bearings was collected in manifolds at the bottom of the test rig and returned to the external system.

The test bearings were lubricated through a number of passages which originated at the bearing ID. Twenty-four passages led directly from the bearing bore to the inner-race surface along the parting plane of the split inner ring. Each inner ring had six additional passages leading from the bore to the land surface on which the cage rides. This combination of passages provided lubricant directly to the balls and to the cage riding-surfaces. The lubrication scheme illustrated in Fig. 27 permits satisfactory bearing operation at 3 million DN.

A parametric study of a lubrication system which includes provision for underrace lubrication and both inner and outer ring cooling is reported in [25]. Typical data from [25] on bearing operating temperatures are shown in Fig. 28 and on bearing power loss in Fig. 29. Underrace lubricant flow is designated as L_i, inner race coolant flow as C_i and outer race coolant flow as C_o. It can be seen from Figs. 28 and 29 that bearing temperature and power loss are complex functions of L_i, C_i and C_o. By varying these flows inner- and outer-race temperatures can be controlled to adjust the thermal gradient, and thus the internal operating conditions, within the bearing. In general, lower bearing temperatures can be achieved only at the expense of higher power loss, but optimum combinations of L_i, C_i and C_o can be worked out.

PROBLEM AREAS

Applications

Large Bearing, Nominally Loaded, 3 Million and Greater DN

Designers of large turbine engines foresee requirements for mainshaft bearings to operate at 3 million DN or higher by the end of this decade. The present operating limit for ball and cylindrical roller bearings is at approximately 2 million DN. Theory predicts a very significant decrease in fatigue life for thrust loaded ball bearings at 3 million DN, due principally to centrifugal effects [1]. As one would expect, bearing operation at 3 million DN also poses severe lubrication and heat removal problems. In ball and cylindrical roller bearings, lubrication and heat removal problems have been solved by the use of:

1. Underrace cooling and centrifugal oil feed directly into the interior of the bearing;
2. Direct centrifugal oil feed to the cage locating surface; and
3. One piece, machined and balanced cages.

In contrast to the problems of lubrication and heat removal which have apparently been solved, it is not yet known whether a solution to the fatigue life problem is in hand. Several approaches are being tried. The increase in stress between the rolling elements and the outer race led naturally to designs incorporating reduced weight balls. Thin wall hollow balls [1 and 118] and drilled balls [116, 117, 119 and 120] have been evaluated experimentally at DN values to 3 million. Flexure failures of both ball types have been encountered. This problem is still being worked on. The drilled ball bearing appears to be the more promising of these approaches;

kinematically it functions very well at 3 million DN, but a ball geometry that is completely free of flexure failures is still being sought.

An interesting aspect of the data obtained in [120] is the comparison between measured and predicted bearing torques. Torques were predicted using the most advanced analysis [81]. The results, shown in Fig. 30, indicate that computed torques were considerably less than those measured. Much work needs to be done to improve torque prediction techniques.

A second approach to the large, ultra-high speed ball bearing problem is the use of hybrid bearings which utilize a fluid film bearing in conjunction with a rolling bearing. The fluid film bearing performs one of two functions: it shares the load as in the parallel hybrid bearing [121], or it shares the speed as in the series hybrid bearing [122]. The parallel hybrid concept is more effective in improving life when the speed is moderate and the load is high because it attenuates system load effects rather than centrifugal effects. In contrast, the series hybrid concept is more effective when the speed is high and the load is moderate because it reduces the operating DN value of the rolling bearing by as much as 40 percent. This results in a significant attenuation of centrifugal effects. An experimental program to evaluate a series hybrid bearing at an equivalent DN value of 3 million is under way.

Improvements in rolling bearing materials (multiple consumable vacuum melting, and forging to produce more favorable fiber orientation) and in surface finishes, together with optimized design, have resulted in bearings with significantly longer fatigue life. Whether the gains in fatigue life achieved through advanced technology are sufficient to offset the

effects of extreme speed has not yet been determined. Full-scale solid ball bearings which incorporate all known technological advances are presently being life tested at 3 million DN. Preliminary results are extremely encouraging; they indicate that satisfactory bearing life may be achieved without resorting to the experimental concepts discussed above.

In cylindrical roller bearings, the effects of high DN values on fatigue life are not as significant as they are in ball bearings, but at least one novel design which reduces roller orbital speed has been evaluated experimentally [123]. In this bearing, dual diameter rollers were used to reduce roller orbital speeds and thus centrifugal effects. The objective of this program is to develop a roller bearing suitable for 3.5 million DN operation.

Large Bearing, Heavily Loaded, 1.5 Million DN

The second application category, that of large bearings operating at DN values to 1.5 million and high combined radial and axial loads, occurs in power transmissions. Until recently, ball and cylindrical roller bearings were used in these applications, but it has been necessary to use duplex sets of as many as four ball bearings in tandem to meet the high load requirements. The proglems with tolerance stackups and poor load sharing in such designs are obvious. Tapered roller bearings are being considered as an alternate bearing type for these applications. The load capacity of tapered roller bearings is adequate for these applications, but conventional designs cannot meet the DN requirements. Therefore, analytical and experimental programs to extend the speed capability of tapered roller bearings have been started [124]. Dynamic analyses to

optimize designs have been completed. These incorporate elastohydrodynamic effects and can be used to predict the influence of design parameters on EHD film thicknesses as well as life. The principal problem is lubrication and heat removal from the contacts between the rollers and the cone rib flange. Much progress has been made, but further work is required before the 1.5 million DN requirement is met. More sophisticated lubrication techniques and perhaps bearing design refinements must be developed.

Small Bearing, Nominally Loaded, 2.5 Million DN

The development of small bore ball and cylindrical roller bearings for service at 2.5 million DN is an especially severe problem. Experience with small bearings has so far been limited to a maximum of 1.8 million DN. The difficulties encountered in operating small bearings at extreme DN values are far greater than those with large bearings, primarily because of:

1. Centrifugal force effects, and
2. Size effects.

DN is a poor severity parameter unless comparisons are limited to a narrow band of bore diameters. Centrifugal effects vary as DN^2 so that in small bearings they can easily be eight times as severe as in large bearings. Two difficulties are immediately apparent: achieving effective lubrication and cooling in the very severe centrifugal force field, and adequate cage strength. Heat removal in a small bearing is more difficult than in a large bearing because the heat generated per unit of surface area is much higher, and because the centrifugal effects on oil particles are more severe.

Because of centrifugal effects, small bore bearings should be designed

with very small balls or rollers. There is a practical limit to this because the annular space available for the cage becomes too small. The cage must be a strong enough structure to withstand both the centrifugal and the rolling-element loads. It is easy to understand why cage problems are common in small bearings, and why they are likely to pose one of the most difficult barriers to overcome in the development of small bearings capable of operating at 2.5 million DN.

Experimental studies of lubrication and cooling techniques, and of various cage designs and materials need to be made. Experiments should be conducted first with ball bearings under pure thrust load and then under combined thrust and radial load. Finally, cylindrical roller bearing tests should be conducted. If conventional bearing concepts cannot be refined to the point of success, hybrid-bearing designs may have to be considered.

CONCLUDING REMARKS

Tremendous progress has been made toward extending rolling-element bearing life and reliability through research on materials and bearing dynamics. Although additional improvements in the resistance of materials to fatigue might still be made, further gains are likely to be less significant than those already achieved, and probably much more costly. The improvements achieved in materials have been startling, and the state of present day bearing material metallurgy is such as to preclude any further huge gains.

Gaps in bearing technology do exist and research to close these gaps is required. Some directions in which research efforts might be directed are:

1. Experimental data on ball, cylindrical and tapered roller bearing dynamics to assess the validity of existing analyses and computer programs.

2. Experimental data on time delay (relaxation) response to Hertzian pressure pulses and on high shear rate effects in very thin (microinches) lubricant films. Much more work needs to be done on lubricant rheology before further significant gains can be made in the prediction of elasto-hydrodynamic film thicknesses and tractive forces.

3. Work on cage materials and designs. The ideal cage material is one with a high strength to weight ratio and a relatively low modulus of elasticity. It should have good strength retention at high temperatures, and good friction and wear characteristics under boundary lubricated sliding. Two piece cage designs which retain their balance at high speeds and under varying ball and roller loads are required.

4. Work on power loss prediction methods needs to be done. This is closely related to a better understanding of fluid rheology and elasto-hydrodynamics, and cage drag forces.

5. Eventually rolling-element or hybrid bearings will be required to function at DN values which may reach 5 million. Innovative designs are required for both ball and roller bearings which attenuate centrifugal effects on contact stresses and power loss. This is perhaps the most challenging area for research on rolling elements.

REFERENCES

1. Harris, T. A., "On the Effectiveness of Hollow Balls in High-Speed Thrust Bearings," ASLE Transactions, Vol. 11, No. 4, Oct. 1968, pp. 290-294. Discussion by P. F. Brown, ASLE Transactions, Vol. 12, No. 3, July 1969, pp. 204-205.

2. Morrison, T. W., Walp, H. O., and Remorenko, R. P., "Materials in Rolling Element Bearings for Normal and Elevated (450° F) Temperature," ASLE Transactions, Vol. 2, No. 1, 1959, pp. 129-146.

3. Bamberger, E. N., "Effect of Materials-Metallurgy Viewpoint," Interdisciplinary Approach to the Lubrication of Concentrated Contacts, SP-237, 1970, NASA, Washington, D. C., pp. 409-437.

4. Carter, T. L., "A Study of Some Factors Affecting Rolling-Contact Fatigue Life," TR R-60, 1960, NASA, Cleveland, Ohio.

5. Bamberger, E. N., "The Effect of Ausforming on the Rolling Contact Fatigue Life of a Typical Bearing Steel," Journal of Lubrication Technology, Vol. 89, No. 1, Jan. 1967, pp. 63-75.

6. Walp, H. O., Remorenko, R. P., and Porter, J. V., "Endurance Tests of Rolling-Contact Bearings of Conventional and High Temperature Steels under Conditions Simulating Aircraft Gas Turbine Applications," WADC TR-58-392, July 1959, SKF Industries, Inc., King of Prussia, Pa.

7. Carter, T. L., Zaretsky, E. V., and Anderson, W. J., "Effect of Hardness and Other Mechanical Properties on Rolling-Contact Fatigue Life of Four High-Temperature Bearing Steels," TN D-270, 1960, NASA, Cleveland, Ohio.

8. Zaretsky, E. V., and Anderson, W. J., "Rolling-Contact Fatigue Studies with Four Tool Steels and a Crystallized Glass Ceramic," Journal of Basic Engineering, Vol. 83, No. 4, Dec. 1961, pp. 603-612.

9. Anderson, W. J., "Performance of 110-mm Bore M-1 Tool Steel Ball Bearings at High Speeds, Loads, and Temperatures," TN 3892, 1957, NACA, Cleveland, Ohio.

10. Carter, T. L., "Preliminary Studies of Rolling-Contact Fatigue Life of High-Temperature Bearing Materials," RM E57K12, 1958, NACA, Cleveland, Ohio.

11. Jackson, E. R., "Rolling-Contact Fatigue Evaluations of Bearing Materials and Lubricants," ASLE Transactions, Vol. 2, No. 1, 1959, pp. 121-128.

12. Scott, D., and Blackwell, J., "Study of the Effect of Material and Hardness Combination on Rolling Contact," Rep. 239, July 1966, National Engineering Lab., Glasgow, Scotland.

13. Parker, R. J., Zaretsky, E. V., and Dietrich, M. W., "Rolling-Element Fatigue Lives of Four M-Series Steels and AISI 52100 at 150° F," TN D-7033, 1971, NASA, Cleveland, Ohio.

14. Parker, R. J., Zaretsky, E. V., and Dietrich, M. W., "Rolling-Element Fatigue Lives of AISI T-1, AISI M-42, AISI 52100, and Halmo at 150° F," TN D-6179, 1971, NASA, Cleveland, Ohio.

15. Parker, R. J., and Zaretsky, E. V., "Rolling-Element Fatigue Lives of Through-Hardened Bearing Materials," Journal of Lubrication Technology, Vol. 94, No. 2, Apr. 1972, pp. 165-173.

16. Bamberger, E. N., and Zaretsky, E. V., "Fatigue Lives at 600° F of 120-mm Bore Ball Bearings of AISI M-50, AISI M-1, and WB-49 Steels," TN D-6156, 1971, NASA, Cleveland, Ohio.

17. Bear, H. R., and Butler, R. H., "Preliminary Metallographic Studies of Ball Fatigue Under Rolling-Contact Conditions," TN 3925, 1957, NACA, Cleveland, Ohio

18. Carter, T. L., Butler, R. H., Bear, H. R., and Anderson, W. S., "Investigation of Factors Governing Fatigue Life with the Rolling-Contact Fatigue Spin Rig," ASLE Transactions, Vol. 1, No. 1, Apr. 1958, pp. 23-32.

19. Jones, A. B., "Metallographic Observations of Ball Bearing Fatigue Phenomena," Symposium on Testing of Bearings, ASTM, 1947, pp. 35-52.

20. Johnson, R. F., and Sewell, J. F., "The Bearing Properties of 1 percent C-Cr Steel as Influenced by Steelmaking Practice," Journal of the Iron and Steel Institute, Vol. 196, Pt. 4, Dec. 1960, pp. 414-444.

21. Cobb, L. D., "Effect of Vacuum Melting on Bearing Steel," Paper presented at the SAE National Passenger Car, Body and Materials Meeting, Detroit, Mich., Mar. 5-7, 1957.

22. Norton, C. E., and Baker, P. S., "The Effect of New Material and Processing Developments on Ball Bearing Fatigue Life," Paper 779B, Jan. 1964, SAE, New York, N. Y.

23. Given, P. S., "Chemical Analysis Variation and Melting Practices," Panel Session, Achievements in AFBMA Calculated Bearing Life, ASME Spring Lubrication Conference, June 1963.

24. Morrison, T. W., Tallian, T., Walp, H. O., and Baile, G. H., "The Effect of Material Variables on the Fatigue Life of AISI 52100 Steel Ball Bearings," ASLE Transactions, Vol. 5, No. 2, Nov. 1962, pp. 347-364.

25. Signer, H., Bamberger, E. N., and Zaretsky, E. V., "Parametric Study of the Lubrication of Thrust Loaded 120-mm Bore Ball Bearings to 3 Million DN," ASME paper to be presented at the ASLE-ASME Lubrication Conference, Atlanta, Ga., Oct. 1973.

26. Baughman, R. A., "Effect of Hardness, Surface Finish, and Grain Size on Rolling-Contact Fatigue Life of M-50 Bearing Steel," Journal of Basic Engineering, Vol. 82, No. 2, June 1960, pp. 287-294.

27. Zaretsky, E. V., Anderson, W. J., and Bamberger, E. N., "Rolling-Element Bearing Life from 400° to 600° F," TN D-5002, 1969, NASA, Cleveland, Ohio.

28. Chevalier, J. L., Dietrich, M. W., and Zaretsky, E. V., "Short-Term Hot Hardness Characteristics of Rolling-Element Steels," TN D-6632, 1972, NASA, Cleveland, Ohio.

29. Chevalier, J. L., Dietrich, M. W., and Zaretsky, E. V., "Hot Hardness Characteristics of Ausformed AISI M-50, Matrix II, WD-65, Modified AISI 440C and Super Nitralloy," TN D-7244, 1973, NASA, Cleveland, Ohio.

30. Chevalier, J. L., Zaretsky, E. V., and Parker, R. J., "A New Criterion for Predicting Rolling-Element Fatigue Lives of Through-Hardened Steels," Paper 72-Lub-32, Oct. 1972, ASME, New York, N. Y.

31. Palmgren, A., Ball and Roller Bearing Engineering 3rd ed., SKF Industries, Philadelphia Pa., 1959, pp. 73-82.

32. Chevalier, J. L., and Zaretsky, E. V., "Effect of Carbide Size, Area, and Density on Rolling-Element Fatigue," TN D-6835, 1972, NASA, Cleveland, Ohio.

33. Bamberger, E. N., et al., "Life Adjustment Factors for Ball and Roller Bearings - An Engineering Design Guide," ASME, New York, 1971.

34. Parker, R. J., Grisaffe, S. J., and Zaretsky, E. V., "Surface Failure of Alumina Balls Due to Repeated Stresses Applied in Rolling Contact at Temperatures to 2000° F," TN D-2274, 1964, NASA, Cleveland, Ohio.

35. Parker, R. J., Grisaffe, S. J., and Zaretsky, E. V., "Rolling-Contact Studies with Four Refractory Materials to 2000° F," ASLE Transactions, Vol. 8, No. 3, July 1965, pp. 208-216.

36. Parker, R. J., Grisaffe, S. J., and Zaretsky, E. V., "Surface Failure of Titanium Carbide Cermet and Silicon Carbide Balls in Rolling Contact at Temperatures to 2000° F," TN D-2459, 1964, NASA, Cleveland, Ohio.

37. Baughman, R. A., and Bamberger, E. N., "Unlubricated High Temperature Bearing Studies," Journal of Basic Engineering, Vol. 85, No. 2, June 1963, pp. 265-272.

38. Wilson, D. S., "Evaluation of Unconventional Lubricants at 1200° F in High-Speed-Rolling Contact Bearings," Paper 61-Lub-9, 1961, ASME, New York, N. Y.

39. Taylor, K. M., Sibley, L. B., and Lawrence, J. C., "Development of a Ceramic Rolling-Contact Bearing for High Temperature Use," Paper 61-Lub-12, 1961, ASME, New York, N. Y.

40. Dee, C. W., "Silicon Nitride Tribological Applications of a Ceramic Material," Tribology, Vol. 3, No. 2, May 1970, pp. 89-92.

41. Parker, R. J., and Zaretsky, E. V., "Rolling-Element Fatigue Life of Silicon Nitride Balls-Preliminary Test Results," TM X-68174, 1972, NASA, Cleveland, Ohio.

42. Zaretsky, E. V., Parker, R. J., and Anderson, W. J., "Effect of Component Differential Hardnesses on Rolling-Contact Fatigue and Load Capacity," TN D-2640, 1965, NASA, Cleveland, Ohio.

43. Zaretsky, E. V., Parker, R. J., and Anderson, W. J., "Component Hardness Differences and Their Effect on Bearing Fatigue," Journal of Lubrication Technology, Vol. 89, No. 1, Jan. 1967, pp. 47-62.

44. Zaretsky, E. V., Parker, R. J., Anderson, W. J., and Reichard, D. W., "Bearing Life and Failure Distribution as Affected by Actual Component Differential Hardness," TN D-3101, 1965, NASA, Cleveland, Ohio.

45. Irwin, A. S., "Effect of Bearing Temperatures on Capacities of Bearings of Various Materials," Paper Presented at ASME Third Spring Lubrication Symposium, New York, N. Y., Mar. 14-15, 1960.

46. Hopkins, J. M., and Johnson, J. H., "Method of Producing Improved Bearing Components by Elimination or Control of Fiber Orientation," NASA CR-55402, Nov. 1963, Marlin-Rockwell Corp., Jamestown, N. Y.

47. Zaretsky, E. V., "The Changing Technology of Rolling-Element Bearings," Machine Design, Vol. 38, No. 24, Oct. 13, 1966, pp. 206-223.

48. Lips, E. M. H., and Van Zuilen, H., "Improved Hardening Technique," Progress, Vol. 66, No. 2, Aug. 1954, pp. 103-104.

49. Schmatz, D. J., and Zackay, V. F., "Mechanical Properties of Deformed Metastable Austenitic Ultrahigh Strength Steels," ASM Transactions, Vol. 51, 1959, pp. 476-494.

50. Justusson, W. M., and Zackay, V. F., "Engineering Properties of Ausformed Steels," Metal Progress, Vol. 82, No. 6, Dec. 1962, pp. 111-114.

51. Marschall, C. W., "Draft Literature Survey on Hot Cold Working of Steel," (AF 33 (657) 9139) Sept. 1962, Battelle Memorial Inst., Columbus, Ohio

52. Koppenaal, T. J., "The Current Status of Thermomechanical Treatment of Steel in the Soviet Union," ASM Transactions, Vol. 62, No. 1, 1969, pp. 24-37.

53. Bamberger, E. N., "The Production, Testing and Evaluation of Ausformed Ball Bearings," AD-637576, June 1966, General Electric Co., Cincinnati, Ohio.

54. Parker, R. J., and Zaretsky, E. V., "Rolling-Element Fatigue Life of Ausformed M-50 Steel Balls," TN D-4954, 1968, NASA, Cleveland, Ohio.

55. Zaretsky, E. V., Parker, R. J., Anderson, W. J., and Miller, S. T., "Effect of Component Differential Hardness on Residual Stress and Rolling-Contact Fatigue," TN D-2664, 1965, NASA, Cleveland, Ohio

56. Cioclov, D., "Discussion to reference 57" Journal of Lubrication Technology, Vol. 91, No. 2, Apr. 1969, pp. 290-293.

57. Foord, C. A., Hingley, C. G., and Cameron, A., "Pitting of Steel Under Varying Speeds and Combined Stresses," Journal of Lubrication Technology, Vol. 91, No. 2, Apr. 1969, pp. 282-290.

58. Lundberg, G., and Palmgren, A., "Dynamic Capacity of Rolling Bearings," Acta Polytechnica, Mechanical Engineering Series, Vol. 1, No. 3, 1947.

59. Zaretsky, E. V., Parker, R. J., and Anderson, W. J., "A Study of Residual Stress Induced During Rolling," Journal of Lubrication Technology, Vol. 91, No. 2, Apr. 1969, pp. 314-319.

60. Akaoka, J., "Some Considerations Relating to Plastic Deformation Under Rolling Contact," Rolling Contact Phenomena, J. B. Bidwell, ed., Elsevier Pub. Co., 1962, pp. 266-300.

61. Gentile, A. J., and Martin, A. D., "The Effects of Prior Metallurgically Induced Compressive Residual Stress on the Metallurgical and Endurance Properties of Overload Tested Ball Bearings," Paper 65-WA/CF-7, Nov. 1965, ASME, New York, N. Y.

62. Scott, R. L., Kepple, R. K., and Miller, M. H., "The Effect of Processing-Induced Near-Surface Residual Stress on Ball Bearing Fatigue," Rolling Contact Phenomena, J. B. Bidwell, ed., Elsevier Pub. Co., 1962, pp. 301-316.

63. Bush, J. J., Grube, W. L., and Robinson, G. H., "Microstructural and Residual Stress Changes in Hardened Steel due to Rolling Contact," Rolling Contact Phenomena, J. B. Bidwell, ed., Elsevier Pub. Co., 1962, pp. 365-399.

64. Almen, J. O., "Effects of Residual Stress on Rolling Bodies," Rolling Contact Phenomena, J. B. Bidwell, ed., Elsevier Pub. Co., 1962, pp. 400-424.

65. Gentile, A. J., Jordan, E. F., and Martin, A. D., "Phase Transformations in High-Carbon, High-Hardness Steels Under Contact Loads," Transactions AIME, Vol. 233, No. 6, June 1965, pp. 1085-1093.

66. Muro, H., and Tsushima, N., "Microstructural, Microhardness and Residual Stress Changes due to Rolling Contact," Wear, Vol. 15, No. 5, May 1970, pp. 309-330.

67. Parker, R. J., and Zaretsky, E. V., "Effect of Residual Stresses Induced by Prestressing on Rolling-Element Fatigue Life," TN D-6995, 1972, NASA, Cleveland, Ohio.

68. Lundberg, G., and Palmgren, A., "Dynamic Capacity of Roller Bearings," Acta Polytechnica, Mechanical Engineering Series, Vol. 2, No. 4, issue 96, 1951.

69. Anon, "Method of Evaluating Load Ratings of Annular Ball Bearings," AFBMA Standards, Section No. 9, Rev. No. 1, Nov. 1950.

70. Harris, T. A., Rolling-Bearing Analysis, Wiley, New York, 1966.

71. Zaretsky, E. V., and Anderson, W. J., "Preliminary Determinations of Temperature Limitations of Ester, Ether, and Hydrocarbon Base Lubricants in 25-MM Bore Ball Bearings," TN D-4146, 1967, NASA, Cleveland, Ohio.

72. Parker, R. J., Bamberger, E. N., and Zaretsky, E. V., "Bearing Torque and Fatigue Life Studies with Several Lubricants for Use in the Range 500° to 700° F," TN D-3948, 1967, NASA, Cleveland, Ohio.

73. Parker, R. J., Bamberger, E. N., and Zaretsky, E. V., "Evaluation of Lubricants for High-Temperature Ball Bearing Applications," Journal of Lubrication Technology, Vol. 90, No. 1, Jan. 1968, pp. 106-112.

74. Bamberger, E. N., Zaretsky, E. V., and Anderson, W. J., "Fatigue Life of 120-MM Bore Ball Bearings at 600° F with Fluorocarbon, Polyphenyl Ether, and Synthetic Base Lubricants," TN D-4850, 1968, NASA, Cleveland, Ohio.

75. Scott, D., "The Effect of Lubricant Viscosity on Ball Bearing Fatigue Life," LDR 44/60, Dec. 1960, Dept. Sci. Ind. Res., National Engineering Lab., Glasgow, Scotland.

76. Dowson, D., and Higginson, G. R., Elasto-Hydrodynamics Lubrications, Pergamon Press, 1966.

77. Jones, A. B., "Ball Motion and Sliding Friction in Ball Bearings," Journal of Basic Engineering, Vol. 81, No. 1, Mar. 1959, pp. 1-12.

78. Harris, T. A., "Ball Motion in Thrust-Loaded Angular Contact Bearings with Coulomb Friction," Journal of Lubrication Technology, Vol. 93, No. 1, Jan. 1971, pp. 32-38.

79. Harris, T. A., "An Analytical Method to Prevent Skidding in Thrust-Loaded Angular Contact Ball Bearings," Journal of Lubrication Technology, Vol. 93, No. 1, Jan. 1971, pp. 17-24.

80. Allen, C. W., Townsend, D. P., and Zaretsky, E. V., "Elastohydrodynamic Lubrication of a Spinning Ball in a Nonconforming Groove," Journal of Lubrication Technology, Vol. 92, No. 1, Jan. 1970, pp. 89-96.

81. Crecelius, W. J., and Harris, T. A., "Ultra-High Speed Ball Bearing Analysis," SKF-AE71A009, NASA CR-120837, Nov. 1971, SKF Industries, Inc., King of Prussia, Pa.

82. Scibbe, H. W., and Zaretsky, E. V., "Advanced Design Concepts for High Speed Bearings," Paper 71-DE-70, 1971, ASME, New York, N. Y.

83. Townsend, D. P., Allen, C. W., and Zaretsky, E. V., "Friction Losses in a Lubricated Thrust-Loaded Cageless Angular-Contact Bearing," TN D-7356, 1973, NASA, Cleveland, Ohio.

84. Townsend, D. P., Allen, C. W., and Zaretsky, E. V., "Study of Ball Bearing Torque Under Elastohydrodynamic Lubrication," Paper 73-Lub-1973, ASME, New York, N. Y.

85. Zaretsky, E. V., and Anderson, W. J., "EHD Lubrication," Machine Design, Vol. 40, No. 26, Nov. 7, 1968, pp. 167-173.

86. McGrew, J. W., Gu, A., Cheng, H. S., and Murray, S. F., "Elastohydrodynamic Lubrication-Preliminary Design Manual," AFAPL-TR-70-27, Nov. 1970, Mechanical Technology, Inc., Latham, N. Y.

87. Valori, R., Sibley, L., and Tallian, T., "Elastohydrodynamic Film Effects on the Load Life Behavior of Rolling Contacts," Paper 65-LUBS-11, 1965, ASME, New York, N. Y.

88. Tallian, T., "On Competing Failure Modes in Rolling Contact," ASLE Transactions, Vol. 10, No. 4, Oct. 1967, pp. 418-439.

89. Skurka, J., "Elastohydrodynamic Lubrication of Roller Bearings," Paper 69-LUB-18, Oct. 1969, ASME, New York, N. Y.

90. Crook, A. W., "The Lubrication of Rollers, II. Film Thickness with Relation to Viscosity and Speed," Philosophical Transactions of the Royal Society of London, Ser. A, Vol. 254, No. 1040, Dec. 1969, pp. 223-237.

91. Sibley, L. B., and Orcutt, F. K., "Elastohydrodynamic Lubrication of Rolling Contact Surfaces," ASLE Transactions, Vol. 4, No. 2, Nov. 1961, pp. 234-249.

92. Christensen, H., "The Lubrication of Rolling Contacts, Measurement of Film Thickness," Acta Polytechnica Scandinovica Mechanical Engineering Series, No. 15, 1963.

93. Dyson, A., Naylor, H., and Wilson, A. R., "The Measurement of Oil-Film Thickness in Elastohydrodynamic Contacts," Proceedings of the Institution of Mechanical Engineers, Vol. 180, Pt. 3B, 1965-1966, pp. 119-134.

94. Parker, R. J., and Kannel, J. W., "Elastohydrodynamic Film Thickness Between Rolling Disks with a Synthetic Paraffinic Oil to 589 K (600° F)," TN D-6411, 1971, NASA, Cleveland, Ohio.

95. Parker, R. J., and Kannel, J. W., "Elastohydrodynamic Film Thickness Measurements with Advanced Ester, Fluorocarbon, and Polyphenyl Ether Lubricants to 589 K (600° F)," TN D-6608, 1971, NASA, Cleveland, Ohio.

96. Grubin, A. N., and Vinogradova, I. A., "Fundamentals of the Hydrodynamic Theory of Heavily Loaded Cylindrical Surfaces," Symposium on Investigation Into the Contact of Machine Components, Book No. 30, Central Scientific Institute for Technology and Mechanical Engineering, Moscow, 1949. (D.S.I.R. Trans. No. 337).

97. Dowson, D., and Higginson, G. R., "A Numerical Solution to the Elasto-Hydrodynamic Problem," Journal of Mechanical Engineering Science, Vol. 1, No. 1, 1959, pp. 7-15.

98. Kannel, J. W., and Bell, J. C., "Interpretations of the Thickness of Lubricant Films in Rolling Contact. 1. - Examination of Measurements Obtained by X-Rays," Journal of Lubrication Technology, Vol. 93, No. 4, Oct. 1971, pp. 478-484.

99. Bell, J. C., and Kannel, J. W., "Interpretations of the Thickness of Lubricant Films in Rolling Contact. 2. - Influence of Possible Rheological Factors," Journal of Lubrication Technology, Vol. 93, No. 4, Oct. 1971, pp. 485-497.

100. Cheng, H. S., "Calculations of Elastohydrodynamic Film Thickness in High Speed Rolling and Sliding Contacts," MTI-67TR-24, AD-652924, May 1967, Mechanical Technology, Inc., Latham, N. Y.

101. Cheng, H. S., "Isothermal Elastohydrodynamic Theory for the Full Range Pressure-Viscosity Coefficient," Journal of Lubrication Technology, Vol. 94, No. 1, Jan. 1972, pp. 35-43.

102. Loewenthal, S. H., and Zaretsky, E. V., "Elastohydrodynamic Analysis Using a Power Law Pressure-Viscosity Relation," TN D-7121, 1973, NASA, Cleveland, Ohio.

103. Cheng, H. S., "A Numerical Solution of Elastohydrodynamic Film Thickness in an Elliptical Contact," Journal of Lubrication Technology, Vol. 92, No. 1, Jan. 1970, pp. 155-162.

104. Loewenthal, S. H., Parker, R. J., and Zaretsky, E. V., "Elastohydrodynamic Film Thickness Model for Heavily Load Contacts," Paper 73 Lub-36, 1973, ASME, New York, N.Y.

105. Rounds, F. G., "Lubricant and Ball Steel Effects on Fatigue Life," Journal of Lubrication Technology, Vol. 93, No. 2, Apr. 1971, pp. 236-245.

106. Parker, R. J., and Zaretsky, E. V., "Effect of Lubricant Extreme-Pressure Additives on Rolling-Element Fatigue Life," TN D-7383, 1973, NASA, Cleveland, Ohio.

107. Townsend, D. P., and Zaretsky, E. V., "Effects of Antiwear and Extreme-Pressure Additives in a Synthetic Paraffinic Lubricant on Ball Spinning Torques," TN D-5820, 1970, NASA, Cleveland, Ohio.

108. Jones, F. C., and Wildock, D. F., "The Mechanism of Lubrication Failure in High-Speed Ball Bearings," ASME Transactions, Vol. 72, No. 6, Aug. 1950, pp. 817-823.

109. Booser, E. R., and Wilcock, D. F., "Minimum Oil Requirements of Ball Bearings," Lubrication Engineering, Vol. 9, No. 3, June 1953, pp. 140-143.

110. Boyd, J., and Eklund, P. R., "Some Performance Characteristics of Ball and Roller Bearings for Aviation Gas Turbines," Paper 51-A-78, 1951, ASME, New York, N. Y.

111. Schuller, F. T., and Anderson, W. J., "Operating Characteristics of 75 Millimeter Bore Ball Bearings at Minimum Oil Flow Rates Over a Temperature Range to 500° F," Lubrication Engineering, Vol. 17, No. 6, June 1961, pp. 291-298.

112. Glenn, D. C., and Anderson, W. J., "Minimum-Oil-Flow Requirements of High-Speed Ball Bearings at Temperatures to 800° F," TN D-1994, 1963, NASA, Cleveland, Ohio.

113. Nemeth, Z. N., and Anderson, W. J., "Effect of Speed Load, and Temperature on Minimum-Oil-Flow Requirements of 30- and 75-Millimeter-Bore Ball Bearings," TN D-2908, 1965, NASA, Cleveland, Ohio.

114. Shim, J., and Leonardi, S. J., "Microfol Lubricant Application System for Advanced Turbine Engine Components - Phase II," NASA CR-120843, June 1972, Mobil Research and Development Corp., Paulsboro, N. J.

115. Macks, E., and Nemeth, Z. N., "Lubrication and Cooling Studies of Cylindrical-Roller Bearings at High Speeds," Rep. 1064, 1952, NACA, Cleveland, Ohio.

116. Coe, H. H., Scibbe, H. W., and Anderson, W. J., "Evaluation of Cylindrically Hollow (Drilled) Balls in Ball Bearings at DN Values to 2.1 Million," TN D-7007, 1970, NASA, Cleveland, Ohio.

117. Holmes, P. W., "Evaluation of Drilled Ball Bearings at DN Values to Three Million. I - Variable Oil Flow Tests," CR-2004 1972, NASA, Washington, D. C.

118. Coe, H. H., Parker, R. J., and Scibbe, H. W., "Evaluation of Electron-Beam Welded Hollow Balls for High-Speed Ball Bearings," Journal of Lubrication Technology, Vol. 93, No. 1, Jan. 1971, pp. 47-59.

119. Holmes, P.W., "Evaluation of Drilled-Ball bearings at DN Values to Three Million. II - Experimental Skid Study and Endurance Tests," CR-2005, 1972, NASA, Cleveland, Ohio.

120. Scibbe, H.W., and Munson, H.E., "Experimental Evaluation of 150-Millimeter Bore Ball Bearings to 3 Million DN Using Either Solid or Drilled Balls," Paper 73-Lub-19, 1973, ASME, New York, N.Y.

121. Wilcock, D.F., and Winn, L.W., "The Hybrid Boost Bearing - A Method of Obtaining Long Life in Rolling Contact Bearing Applications," Journal of Lubrication Technology, Vol. 92, No. 3, July 1970, pp. 406-412.

122. Anderson, W.J., Fleming, D.P., and Parker, R.J., "The Series Hybrid Bearing - A New High Speed Bearing Concept," Journal of Lubrication Technology, Vol. 94, No. 2, Apr. 1972, pp. 117-124.

123. Rumberger, J.H., Filetti, E., Dunfee, J., and Gubernick, D., "Dual Diameter Roller Bearing - 3.5 Million DN - 600° F," FIRL-F-C 3132, AFAPL-TR-7323, AD-760563, May 1973, Franklin Institute Research Labs, Philadelphia, Pa.

124. Crecelins, W.J., and Milke, D.R., "Dunamic and Thermal Analysis of High Speed Tapered Roller Bearings Under Combined Loadings," SKF-AL73P010, NASA CR-121207, Mar. 1973, SKF Industries, Inc., King of Prussia, Pa.

TABLE I. - EHD AND MATERIAL HARDNESS EFFECTS ON RELATIVE FATIGUE LIFE OF 120-MM ANGULAR-CONTACT BALL BEARINGS AT THREE TEMPERATURES [27]. [Material, AISI M-50 steel; maximum Hertz stress, 323 000 psi (233 N/cm^2); contact speed, 9760 fpm (4958 cm/sec); lubricant, synthetic paraffinic oil with antiwear and antifoam additives.]

Temperature		Nominal Rockwell C hardness at temperature	Relative life			
°F	K		Experimental 10-percent life	Predicted life from EHD film thickness	Predicted life from hardness differences	Predicted life from combined EHD and hardness effects
400	478	60	1.2	1.3	1.3	1.6
500	533	59	1.6	1.1	1.1	1.3
600	588	58	1	1	1	1

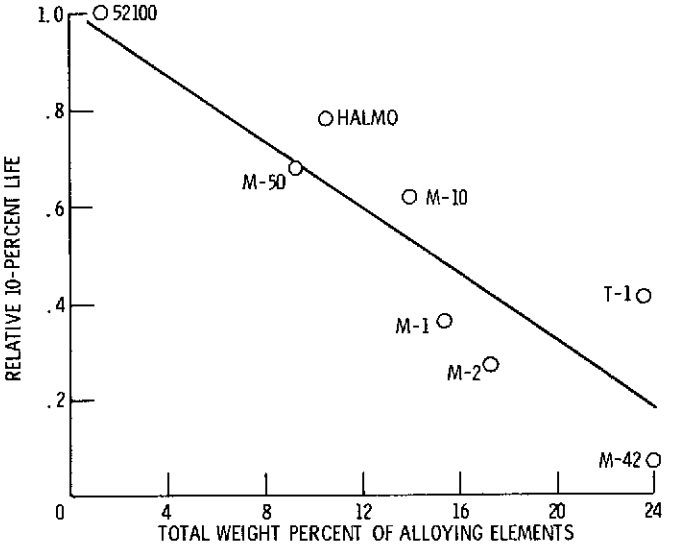

Figure 1. - Effect of total weight percent of alloying elements tungsten, chromium, vanadium, molybdenum, and cobalt on rolling-element fatigue life at 150° F.

CS-67902

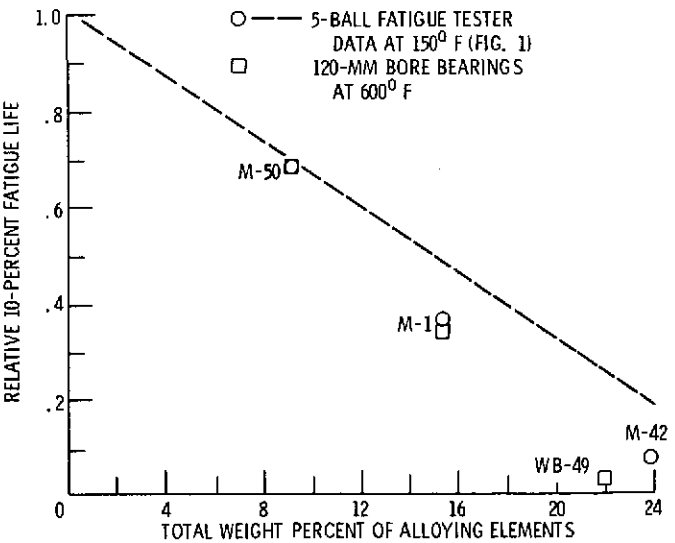

Figure 2. - Effect of total weight percent of alloying elements on fatigue life of 120-mm bore bearings at 600° F.

CS-67903

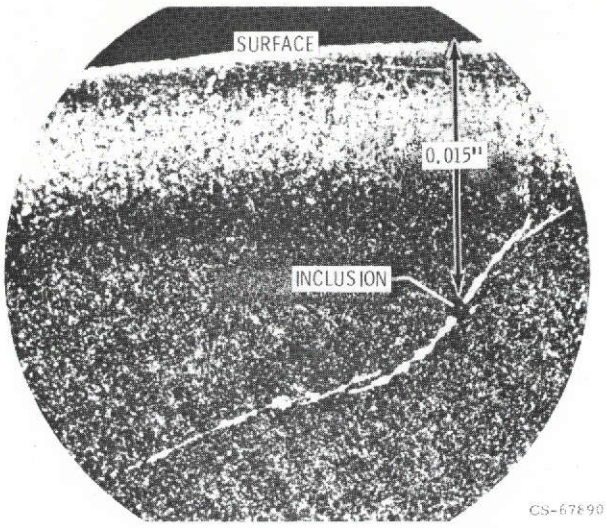

Figure 3. - Fatigue crack emanating from an inclusion.

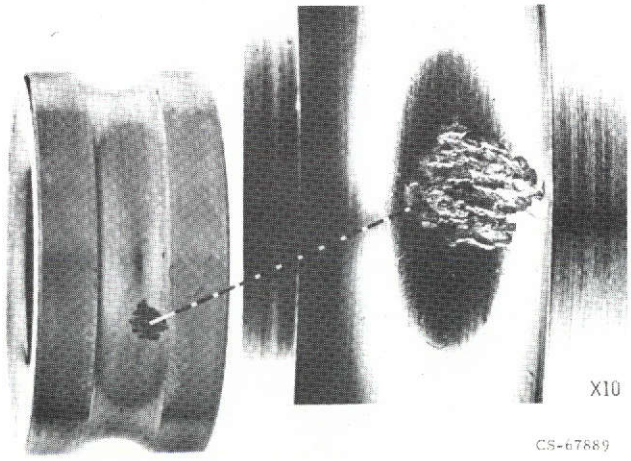

Figure 4. - Typical fatigue spall in bearing race.

This page is reproduced at the back of the report by a different reproduction method to provide better detail.

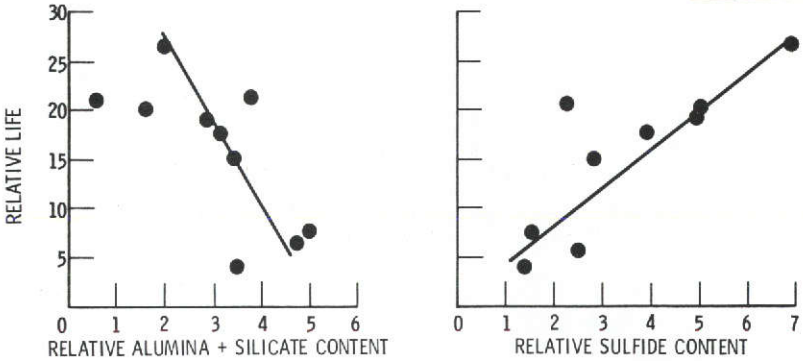

Figure 5. - Relationship between life and inclusion content.

CS-67901

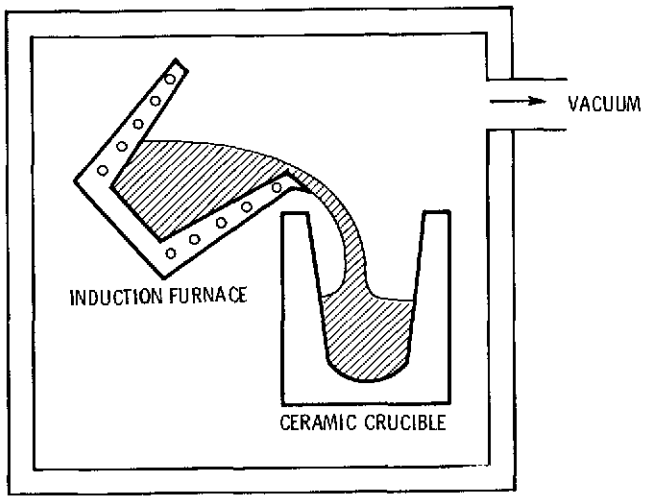

Figure 6. - Induction vacuum melting.

CS-67900

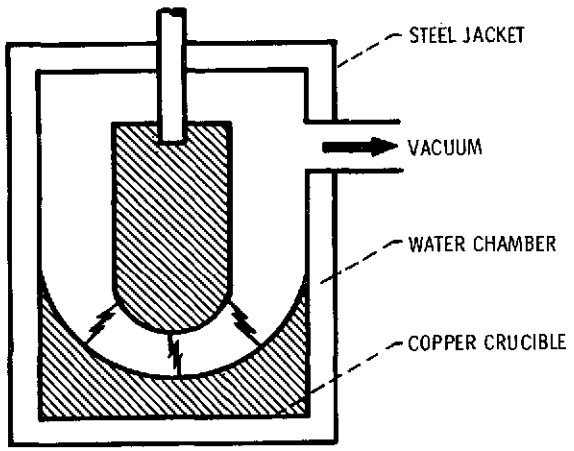

Figure 7. - Consumable electrode vacuum melting.

CS-67899

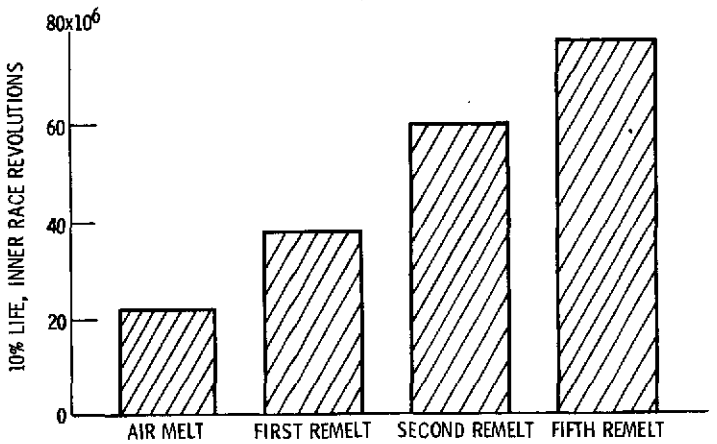

Figure 8. - Life of 6309-size bearing inner races made from air melt and successive consumable remelts of the same heat AISI 52100 steel.

CS-67898

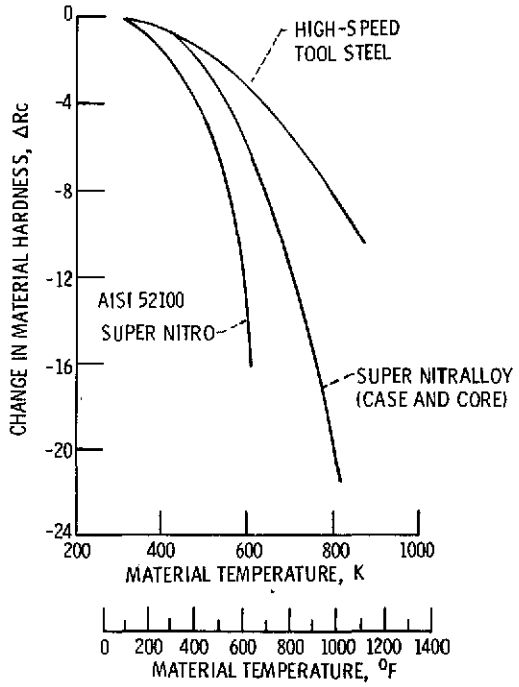

Figure 9. - Normalized short-term hot hardness as a function of temperature.

CS-67897

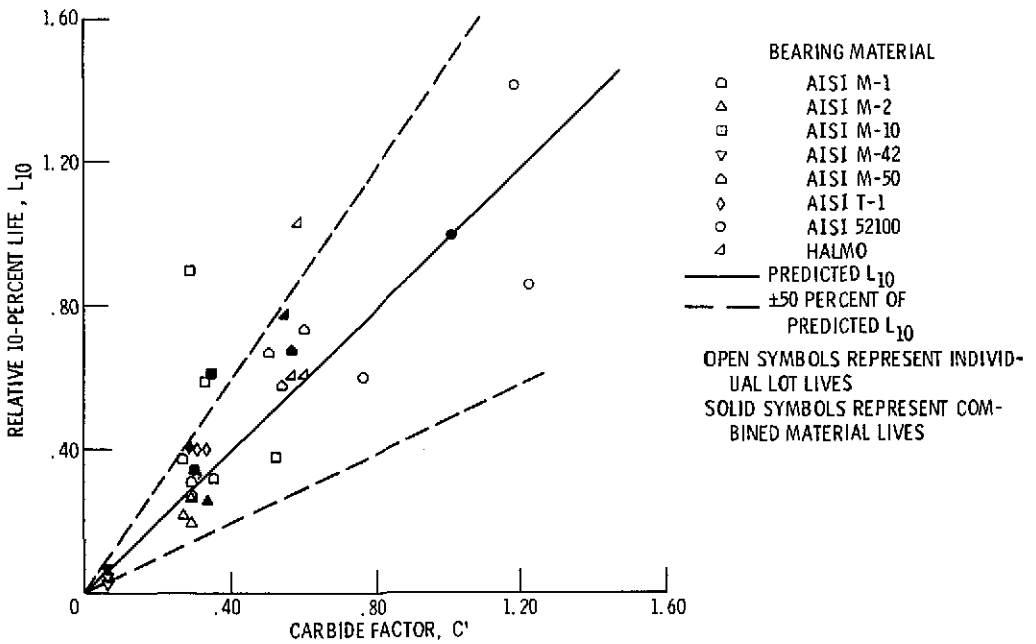

Figure 10. - Individual and combined 10-percent life for eight bearing materials as a function of the carbide factor, C'.

CS-67912

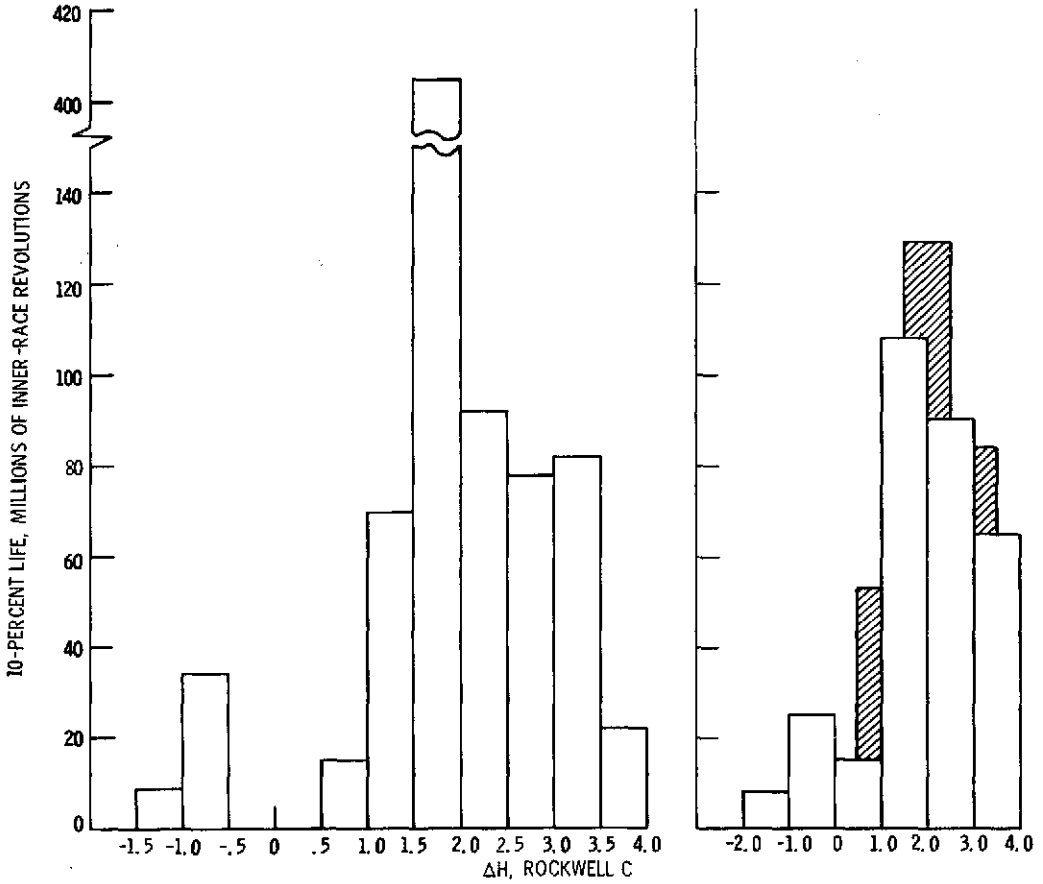

(a) ACTUAL ΔH INCREMENT, 0.5.

(b) ACTUAL ΔH INCREMENT, 1.0.

Figure 11. - Ten-percent life as function of ΔH (difference in Rockwell C hardness balls and races) for AISI 52100 207-size deep-groove ball bearings.

CS-67917

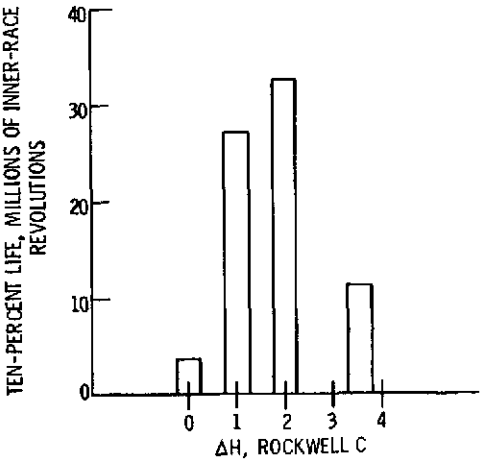

Figure 12. - Ten-percent life as function of ΔH (difference in Rockwell C hardness between balls and races) for AISI 52100 207-S size deep-groove ball bearings.

CS-67895

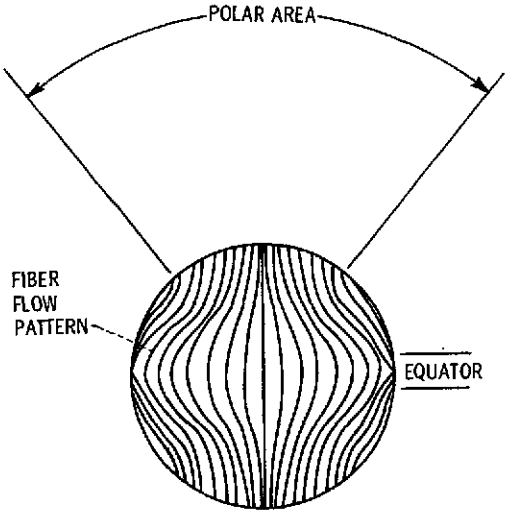

Figure 13. - Fiber orientation in a bearing ball.

CS-67896

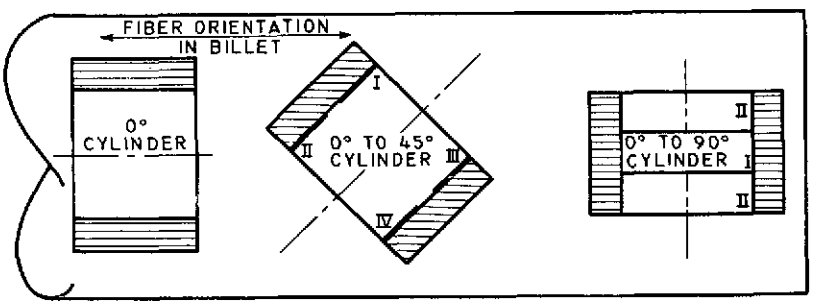

Figure 14. - T-1 tool steel cylinder orientation in billet stock.

CS-67904

E-7697

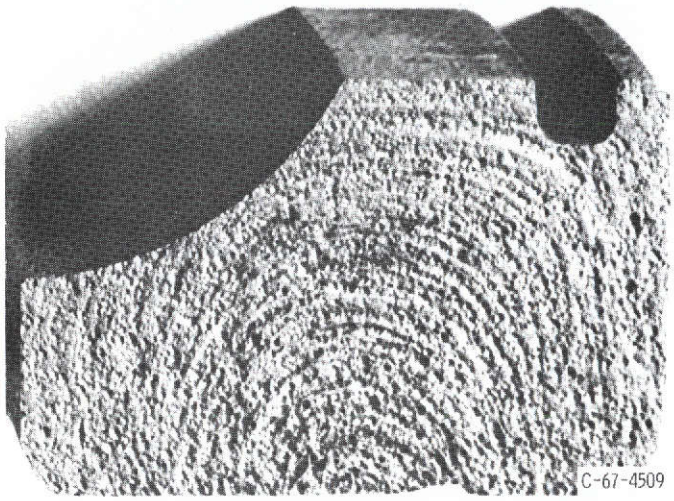

Figure 15. - Bearing race showing fiber flow primarily perpendicular to raceway.

CS-67892

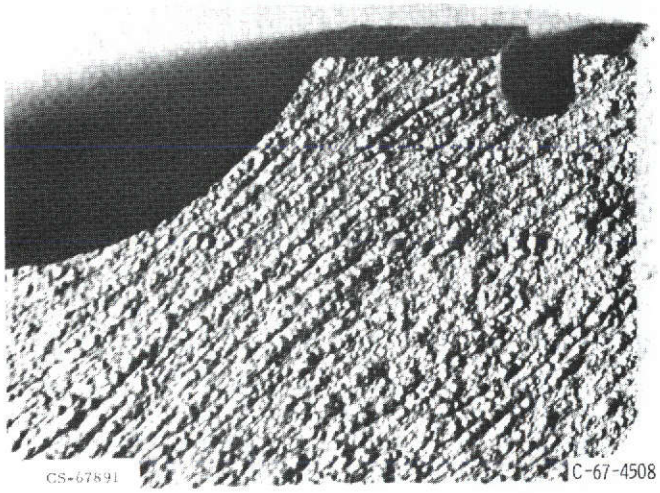

Figure 16. - Forged bearing race showing fiber flow parallel to raceway.

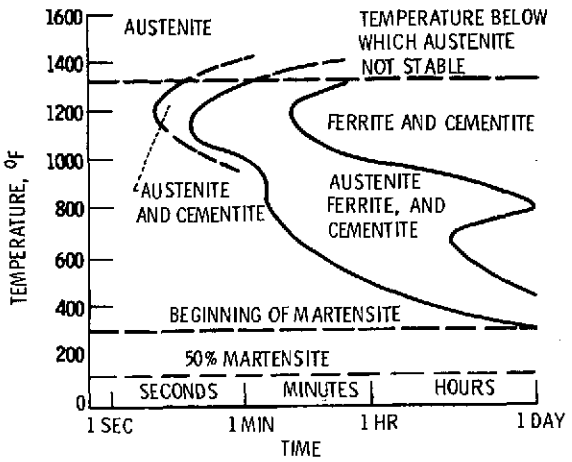

Figure 17. - Time-temperature-transformation curve for SAE 52100. (Absence of "Bay" region makes this material unsuitable for ausforming.)

CS-67906

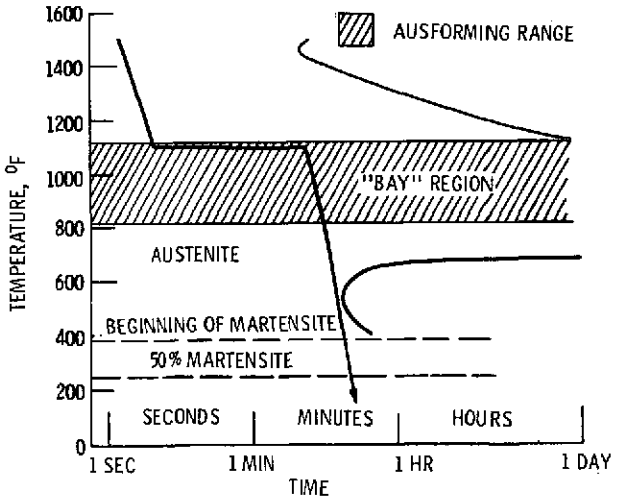

Figure 18. - Time temperature-transformation curve for a typical "M"-type bearing steel ("Bay" or hold region makes this type of steel suitable for ausforming. Arrow indicates ausforming cycle.)

CS-67905

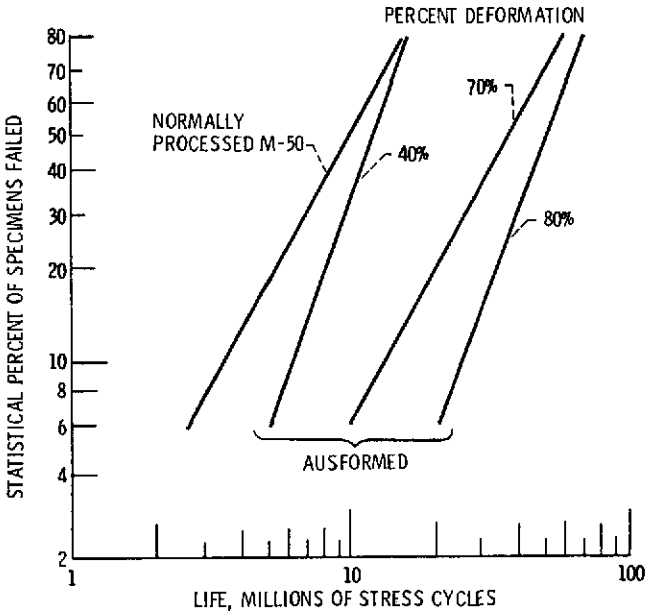

Figure 19. - Effect of ausforming on fatigue life for M-50 bearing steel.

CS-67907

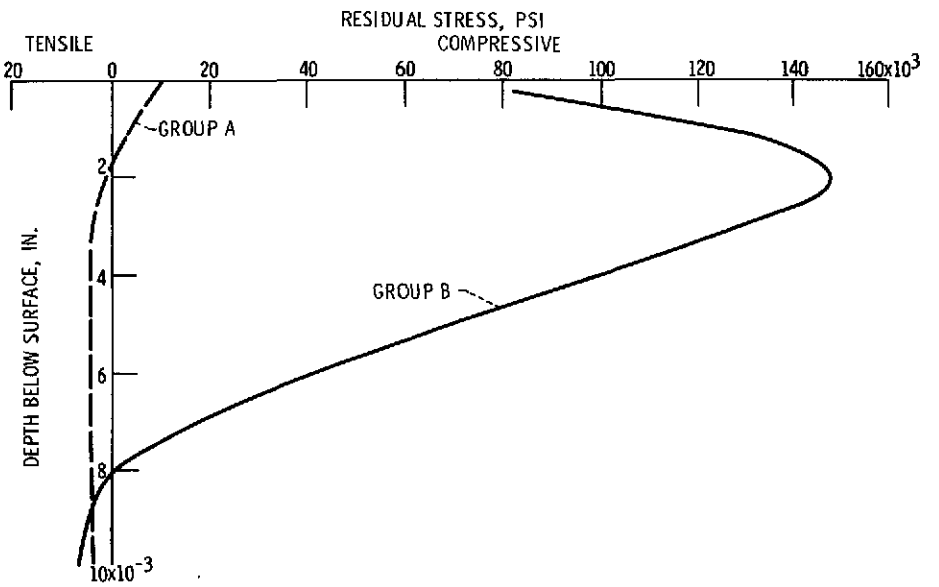

Figure 20. - Tangential residual stress patterns for two groups of 40 mm bore-size bearing races.

CS-67908

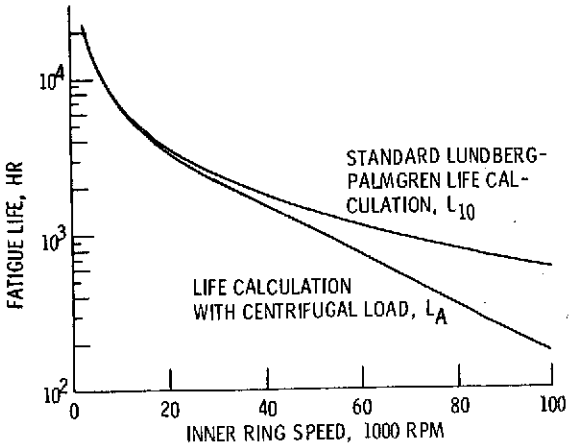

Figure 21. - Comparison of fatigue life of 20-mm-bore ball bearings with 100-lb radial load with and without centrifugal effects considered.

CS-67893

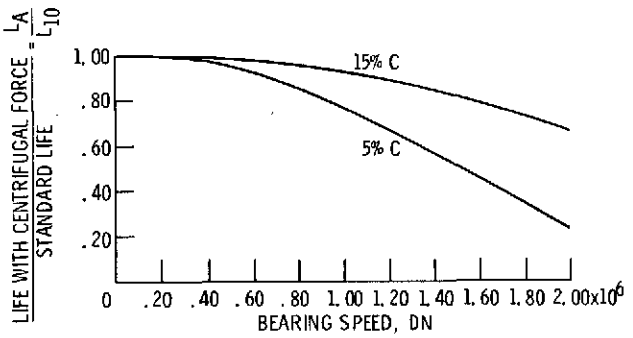

Figure 22. - Effect of speed on bearing life for 20-mm-bore ball bearings.

CS-67894

E-7697

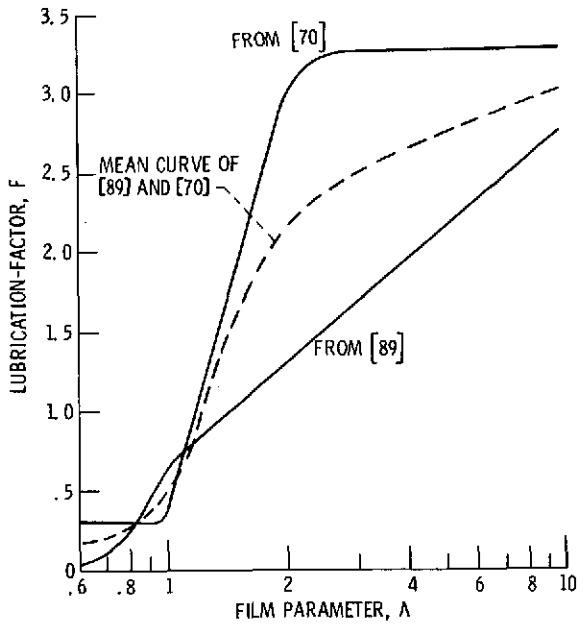

Figure 23. - Lubrication factor, F as function of film parameter, Λ.

CS-67909

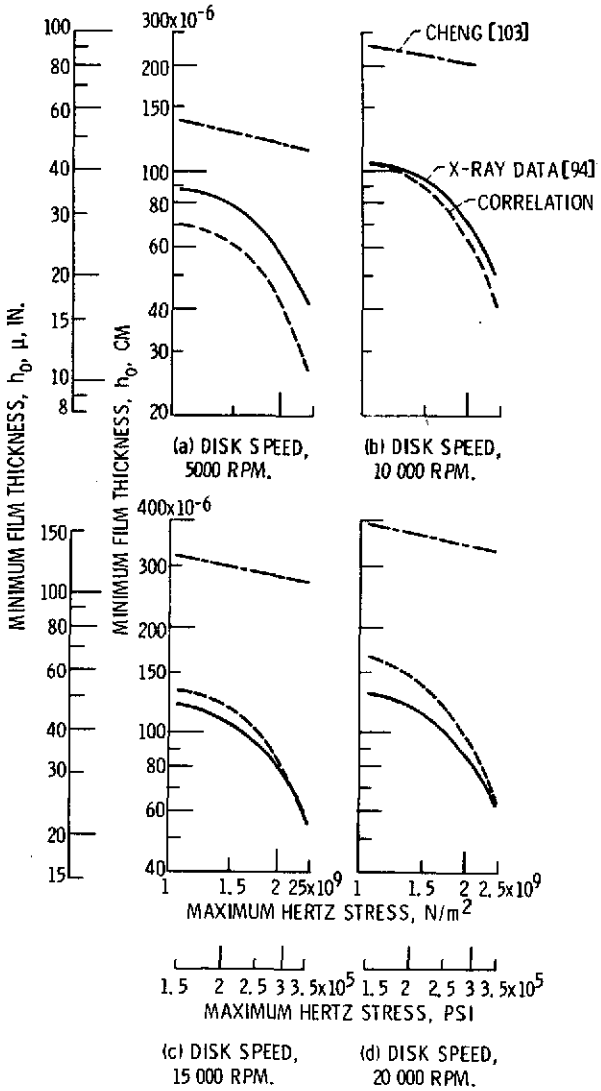

Figure 24. - Comparison of predicted minimum film thickness with X-ray data for a synthetic paraffinic oil at T_0 = 339 K (150° F).

CS-67914

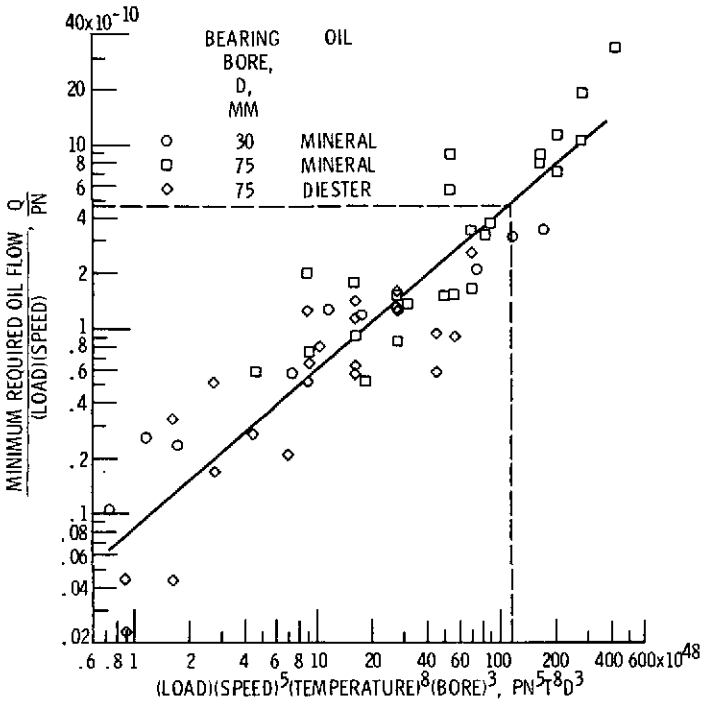

Figure 25. - Generalized correlation of minimum-required-oil-flow data for two bearing sizes and two lubricants. DN range, 0.6×10^6 to 0.975×10^6; thrust load range, 26 to 3000 pounds; bearing temperature range, 225^0 to 500^0 F. Example (dashed line): load, P, 265 pounds; speed, N, 30 000 rpm; bearing temperature, T, 400^0 F; bearing bore, D, 30 millimeters; $PN^5T^8D^3 = 114 \times 10^{48}$; $Q/PN = 4.65 \times 10^{-10}$; minimum required oil flow, Q, 3.7×10^{-3} pounds per minute.

CS-67913

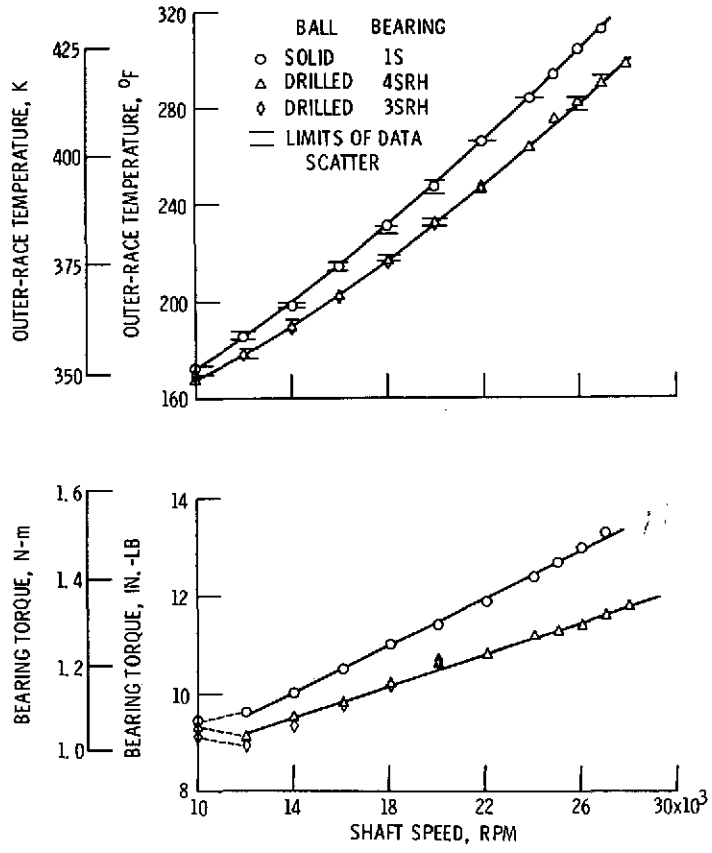

(a) OIL-AIR MIST LUBRICATION AT 0.01 TO 0.07 POUNDS PER MINUTE.

Figure 26. - Comparison of bearing torques and temperatures' with oil-air mist and oil jet lubrication. 75 mm bore ball bearings; solid and drilled balls.

CS-67915

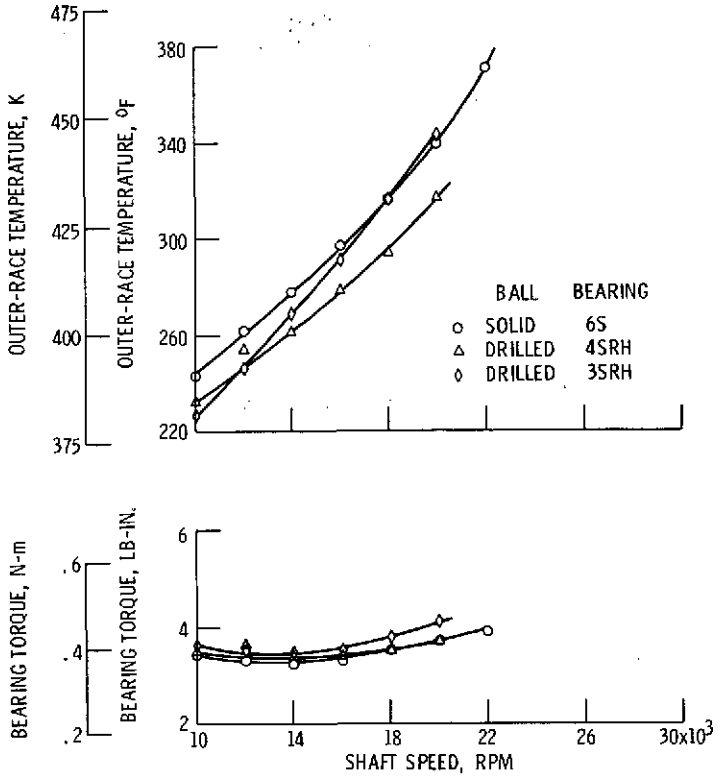

(b) OIL JET LUBRICATION AT 0.95 POUNDS PER MINUTE.

Figure 26. - Concluded.

CS-67916

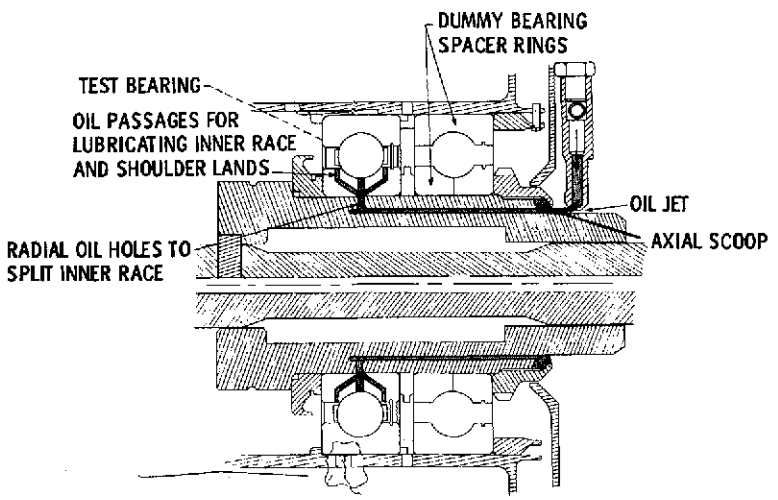

Figure 27. - Under race bearing lubrication. CS-67910

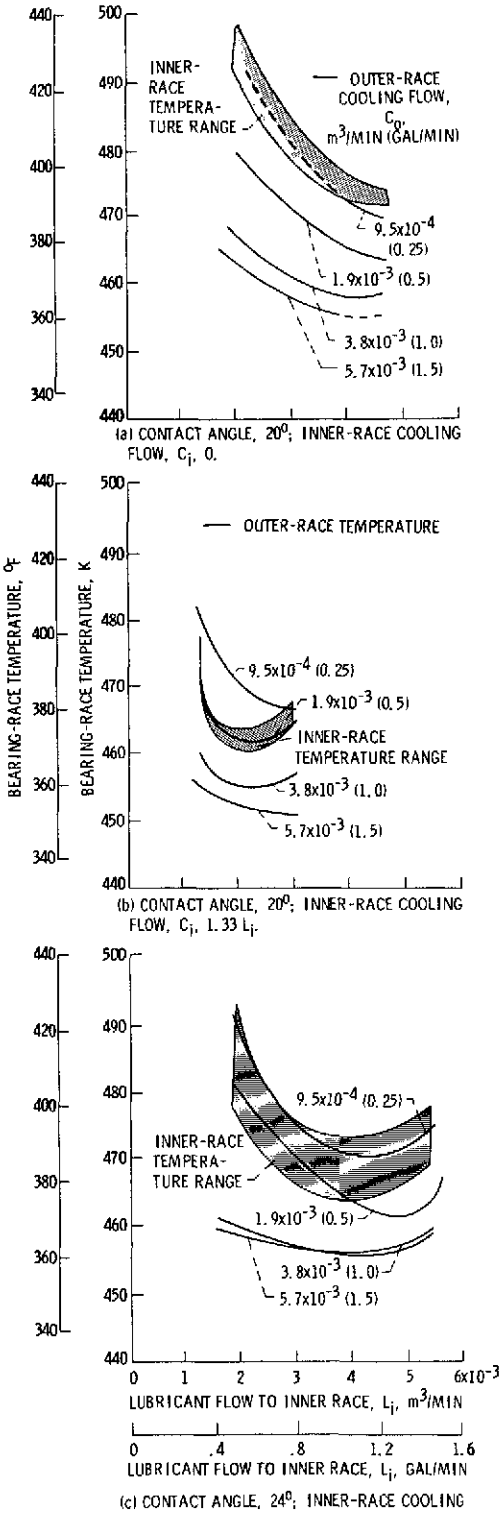

Figure 28. - Bearing race temperature as a function of lubricant flow into bearing, L_i, for varying inner (C_i) and outer (C_o) race cooling rates. Bearing type, 120-mm bore angular-contact ball bearing; bearing thrust load, 22 241 N (5000 lb); speed, 25 000 rpm ($3x10^6$ DN); oil inlet temperature, 394 K (250° F).

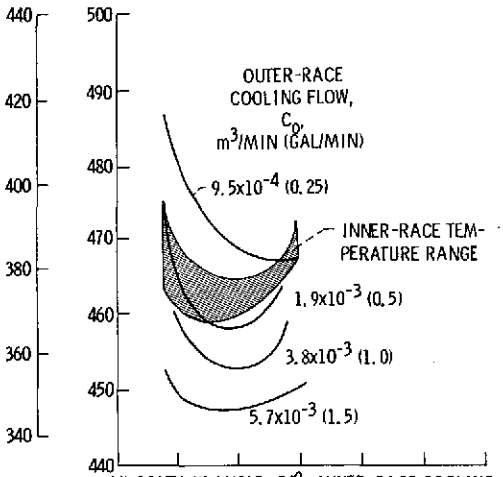

(d) CONTACT ANGLE, 24°; INNER-RACE COOLING FLOW, C_i, 1.33 L_i.

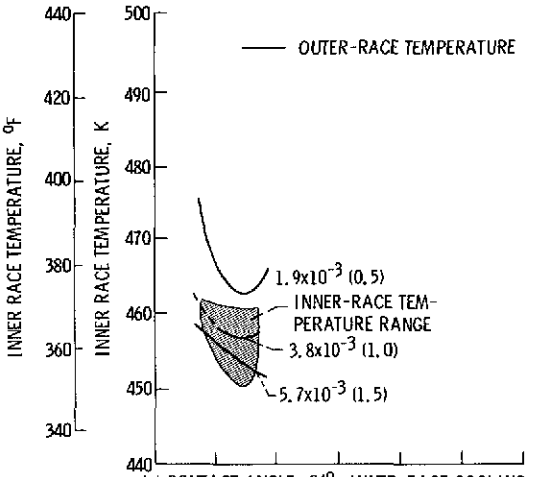

(e) CONTACT ANGLE, 24°; INNER-RACE COOLING FLOW, C_i, 3 L_i.

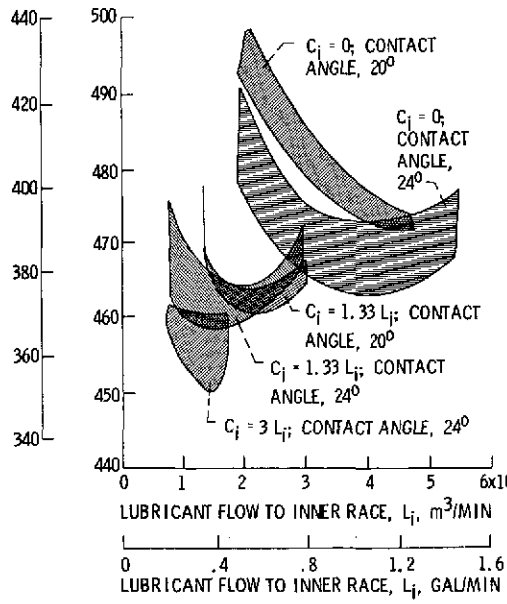

(f) SUMMARY OF INNER-RACE TEMPERATURES.

Figure 28. - Concluded.

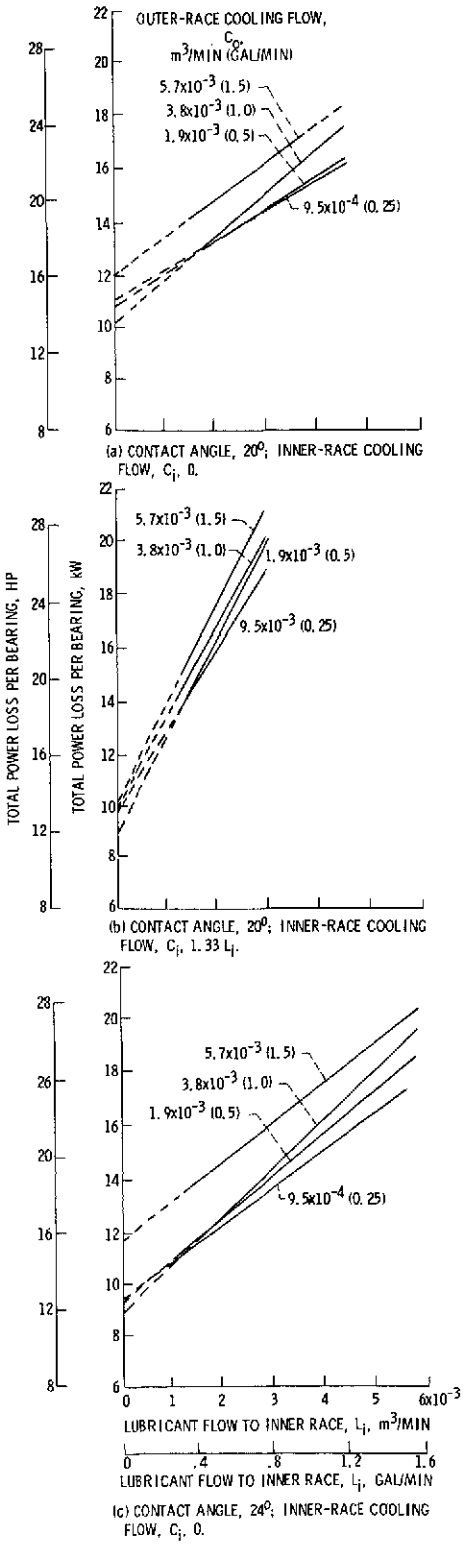

(a) CONTACT ANGLE, 20°; INNER-RACE COOLING FLOW, C_i, 0.

(b) CONTACT ANGLE, 20°; INNER-RACE COOLING FLOW, C_i, 1.33 L_i.

(c) CONTACT ANGLE, 24°; INNER-RACE COOLING FLOW, C_i, 0.

Figure 29. - Bearing power loss as a function of lubricant flow into bearing, L_i, for varying inner (C_i) and outer (C_o) race cooling rates. Bearing type, 120-mm bore angular-contact ball bearing; bearing thrust load, 22 241 N (5000 lb); speed, 25 000 rpm ($3x10^6$ DN); oil inlet temperature, 394 K (250° F).

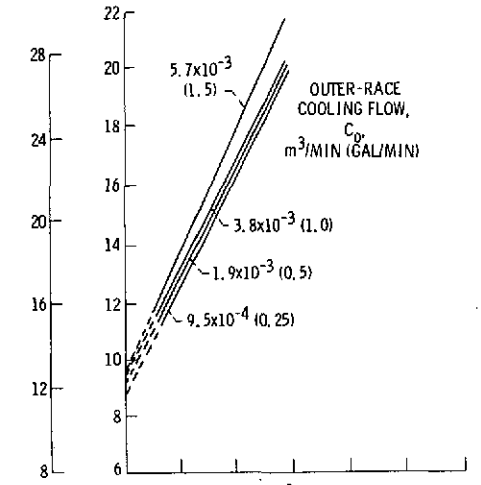

(d) CONTACT ANGLE, 24°; INNER-RACE COOLING FLOW, C_i, 1.33 L_i.

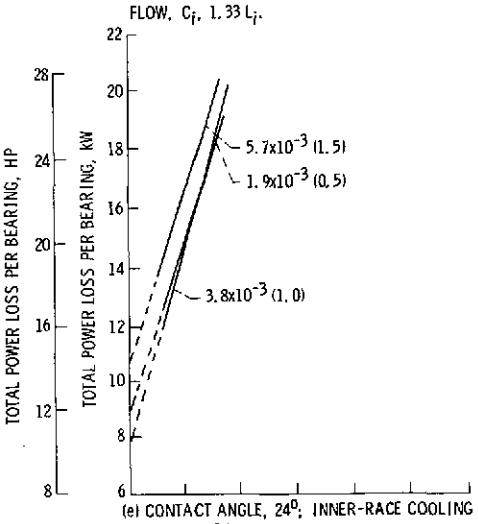

(e) CONTACT ANGLE, 24°; INNER-RACE COOLING FLOW, C_i, 3 L_i.

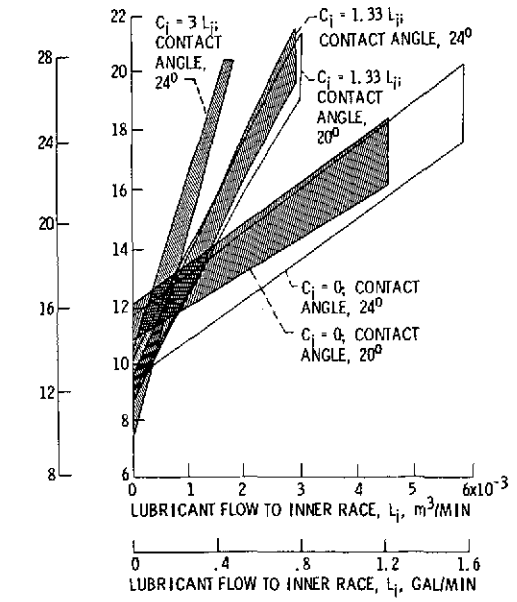

(f) SUMMARY OF BEARING POWER LOSSES.

Figure 29. - Concluded.

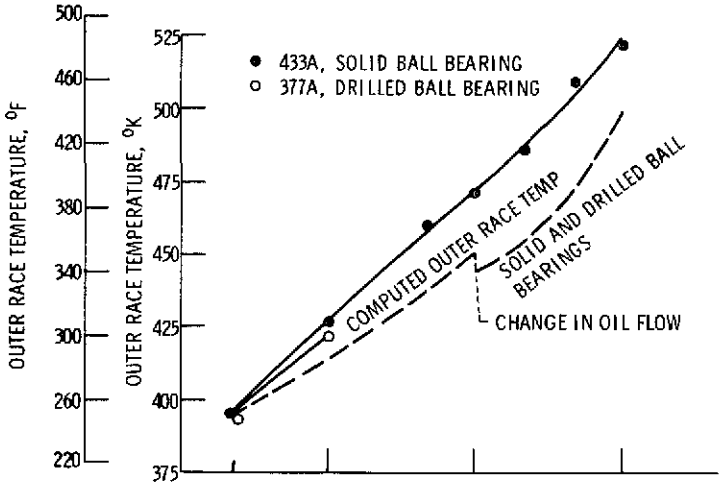

(a) OUTER RACE TEMPERATURE.

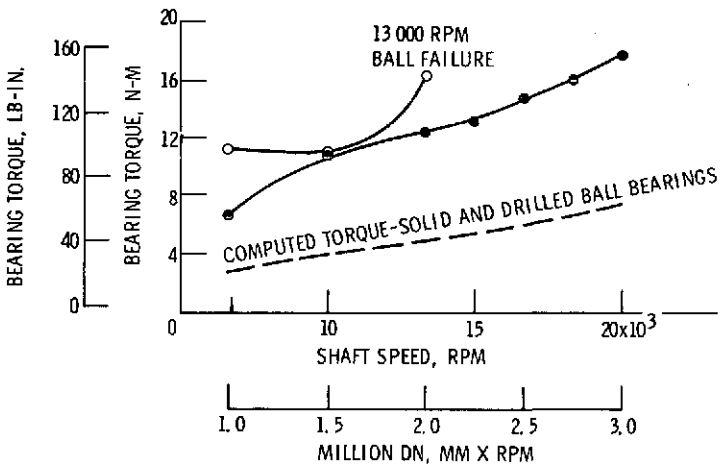

(b) BEARING TORQUE.

Figure 30. - Bearing outer-race temperature and torque as a function of shaft speed at 17 800 newton (4000 lb) thrust load. Type II ester oil MIL-L-23699 at 367° K (200° F) oil inlet temperature. Oil flow 4.35 and 5.80 liters/min (1.15 and 1.57 gpm). CS-67911